Introduction to the spectral function approach

Artur M. Ankowski
SLAC, Stanford University

Testing and Improving Models
of Neutrino-Nucleus Interactions in Generators
ECT*, Trento, June 3−7, 2019

Outline

- **Impulse approximation**
- **Fermi gas model**
- **Shell model**
- **Spectral function approach**

Impulse approximation

Impulse approximation

Assumption: the dominant process of lepton-nucleus interaction is **scattering off a single nucleon**, with the remaining nucleons acting as a spectator system.

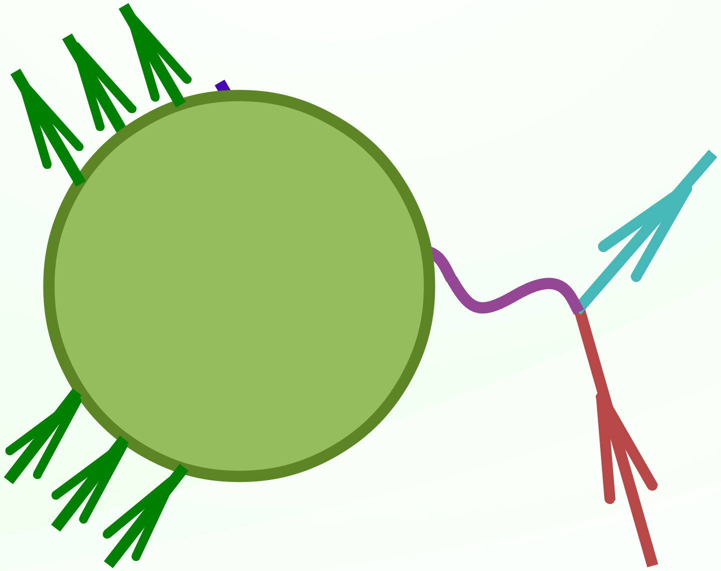

Impulse approximation

Assumption: the dominant process of lepton-nucleus interaction is **scattering off a single nucleon**, with the remaining nucleons acting as a spectator system.

It is valid when the momentum transfer |**q**| is high enough, as the probe's spatial resolution is ~1/|**q**|.

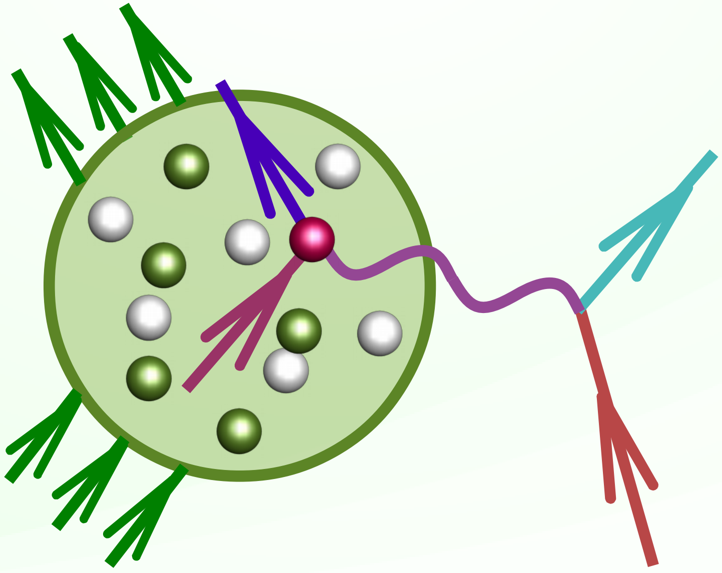

Impulse approximation

$$\frac{d\sigma_{\ell A}}{d\omega d\Omega} = \sum_N \int d\omega'\, d^3p\, dE\, \underline{P^N_{\text{hole}}(\mathbf{p},E)}\, \underline{\frac{M}{E_{\mathbf{p}}}\frac{d\sigma^{\text{elem}}_{\ell N}}{d\omega' d\Omega}}\, \underline{P^N_{\text{part}}(\mathbf{p}',\mathcal{T}',\omega')}$$

Hole spectral function

Particle spectral function

Elementary cross section

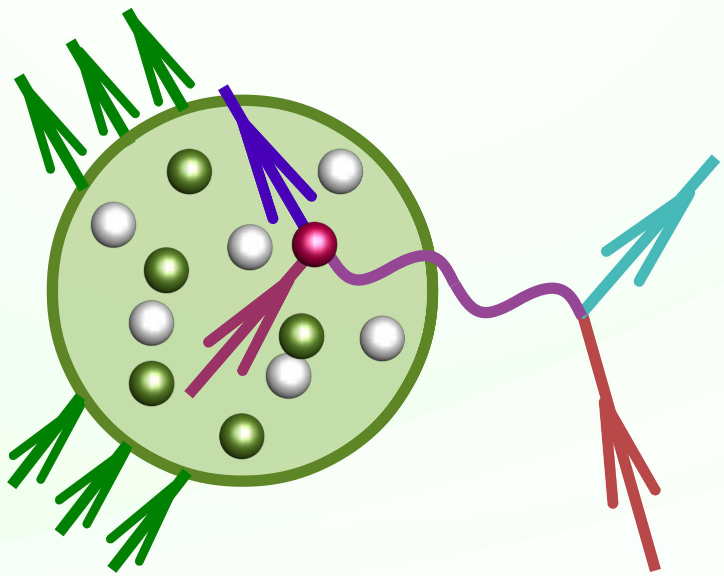

Impulse approximation

$$\frac{d\sigma_{\ell A}}{d\omega d\Omega} = \sum_N \int d\omega'\, d^3p\, dE\; \underline{P^N_{\mathrm{hole}}(\mathbf{p}, E)}\; \frac{M}{E_{\mathbf{p}}} \frac{d\sigma^{\mathrm{elem}}_{\ell N}}{d\omega' d\Omega} P^N_{\mathrm{part}}(\mathbf{p}', \mathcal{T}', \omega')$$

Describes the ground-state properties of the target nucleus

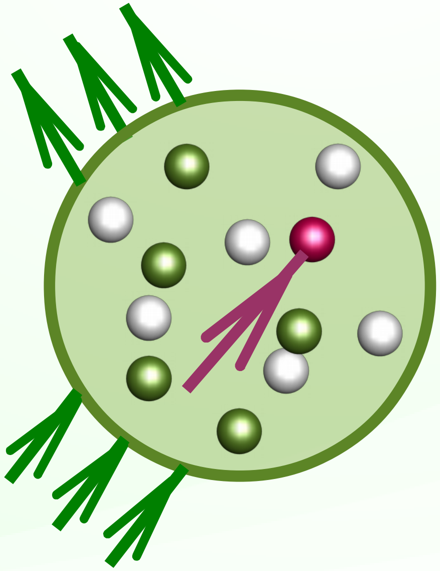

Impulse approximation

$$\frac{d\sigma_{\ell A}}{d\omega d\Omega} = \sum_N \int d\omega'\, d^3p\, dE\, P^N_{\rm hole}(\mathbf{p}, E)\, \underline{\frac{M}{E_{\mathbf{p}}} \frac{d\sigma^{\rm elem}_{\ell N}}{d\omega' d\Omega}}\, P^N_{\rm part}(\mathbf{p}', \mathcal{T}', \omega')$$

Characterizes the interaction vertex

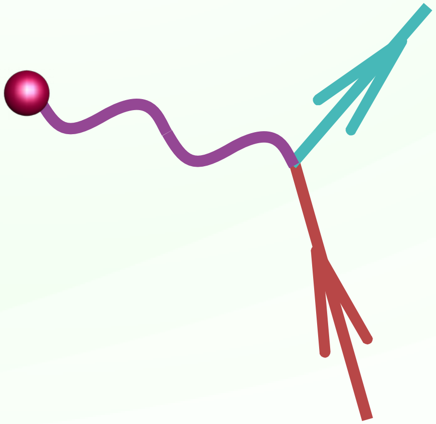

Impulse approximation

$$\frac{d\sigma_{\ell A}}{d\omega d\Omega} = \sum_N \int d\omega' \, d^3p \, dE \, P^N_{\text{hole}}(\mathbf{p}, E) \, \frac{M}{E_{\mathbf{p}}} \frac{d\sigma^{\text{elem}}_{\ell N}}{d\omega' d\Omega} \, \underline{P^N_{\text{part}}(\mathbf{p}', \mathcal{T}', \omega')}$$

Ensures the energy conservation and Pauli blocking

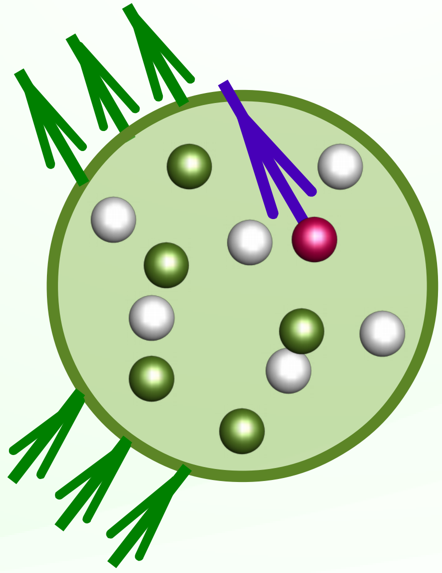

Off-shell effects

Consider a nucleus stable against emission of nucleons.

As in its ground state, $E_A = M_A$, the energy cannot be decreased by emission of a nucleon

$$E_A = E_{A-1} + E_p < E_{A-1} + M$$

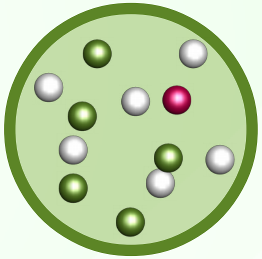

so the energy of a nucleon in the nucleus is lower than M.

V.R. Pandharipande, Nucl. Phys. B (Proc. Suppl.) 112, 51 (2002)

Off-shell effects

In a nuclear model, the initial nucleon's energy may

- differ from the on-shell energy by a constant

$$\boxed{E_p = \sqrt{M^2 + |\mathbf{p}|^2} - \epsilon}$$

- be a function of the momentum

$$\boxed{E_p = \sqrt{M^2 + |\mathbf{p}|^2} - \varepsilon(|\mathbf{p}|)}$$

- lack 1:1 correspondence with momentum

increasing sophistication

Off-shell effects

The elementary cross section,

$$\boxed{\frac{d\sigma^{\text{elem}}_{\ell N}}{dE_{\mathbf{k}'}d\Omega dE_{\mathbf{p}'}d\Omega_{\mathbf{p}'}} \propto L_{\mu\nu}H^{\mu\nu}}$$

contains two tensors

$$\boxed{L_{\mu\nu} \propto j^{\text{lept}}_{\mu} j^{\text{lept}*}_{\nu} \quad \text{and} \quad H^{\mu\nu} \propto j^{\mu}_{\text{hadr}} j^{\nu *}_{\text{hadr}}}$$

with **only the hadron one** affected by off-shell effects.

Off-shell effects

The current appearing in the hadron tensor is known on the mass shell,

$$j^\mu_{\rm hadr} = \overline{u}(\mathbf{p}', s') \left(\gamma^\mu F_1 + i\sigma^{\mu\kappa} \frac{q_\kappa}{2M} F_2 + \ldots \right) u(\mathbf{p}, s)$$

or equivalently

$$j^\mu_{\rm hadr} = \overline{u}(\mathbf{p}', s') \left(\gamma^\mu (F_1 + F_2) - \frac{(p + p')^\mu}{2M} F_2 + \ldots \right) u(\mathbf{p}, s)$$

Off-shell effects

The prescription of de Forest [NPA 392, 232 (1983)]:

to approximate the off-shell hadron tensor, one can use the on-shell expression with the same momentum transfer and a modified energy transfer,

$$\boxed{H^{\mu\nu}_{\text{off-shell}}(p,q) \to H^{\mu\nu}_{\text{off-shell}}(\tilde{p},\tilde{q})}$$

with

$$\boxed{\tilde{p} = (\sqrt{M^2+\mathbf{p}^2}, \mathbf{p}) \quad \text{and} \quad \tilde{q} = (\tilde{\omega}, \mathbf{q})}$$

Off-shell effects

The prescription of de Forest [NPA 392, 232 (1983)]:

as the initial nucleon's energy is now $E_{\boldsymbol{p}} = \sqrt{M^2 + \boldsymbol{p}^2}$
in our calculations, and the final energy is an observable,
the energy transfer has to be

$$\boxed{\tilde{\omega} = \sqrt{M^2 + (\mathbf{p} + \mathbf{q})^2} - \sqrt{M^2 + \mathbf{p}^2}}$$

the difference between the “lepton” ω and “hadron” $\widetilde{\omega}$
is transferred to the spectator system of (A-1) nucleons.

Off-shell effects

Examples of an oversimplified treatment:

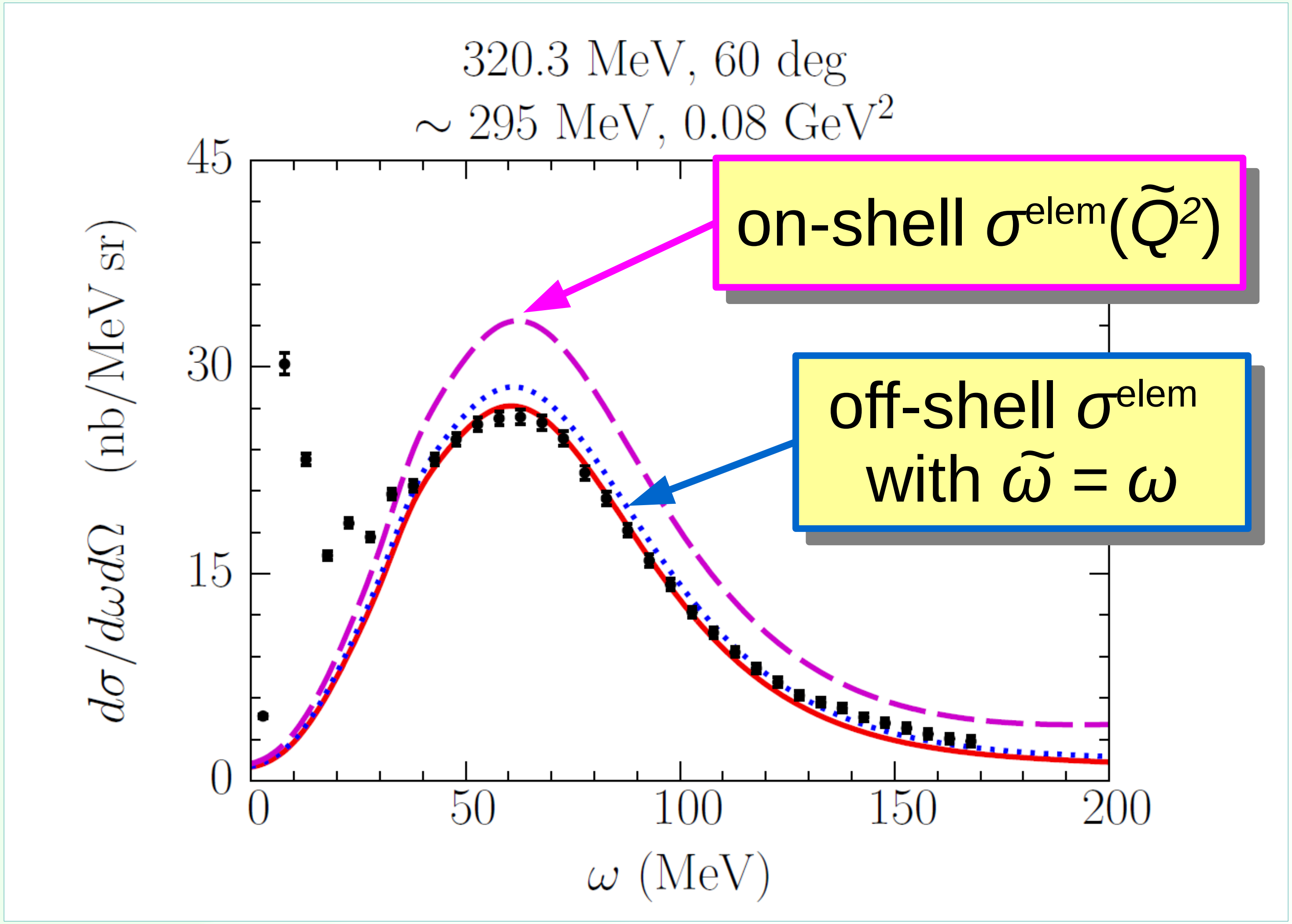

Impulse approximation

$$\frac{d\sigma_{\ell A}}{d\omega d\Omega} = \sum_N \int d\omega'\, d^3p\, dE\, P^N_{\mathrm{hole}}(\mathbf{p}, E)\, \frac{M}{E_{\mathbf{p}}}\, \frac{d\sigma^{\mathrm{elem}}_{\ell N}}{d\omega' d\Omega}\, P^N_{\mathrm{part}}(\mathbf{p}', \mathcal{T}', \omega')$$

Hole spectral function

Particle spectral function

Elementary cross section

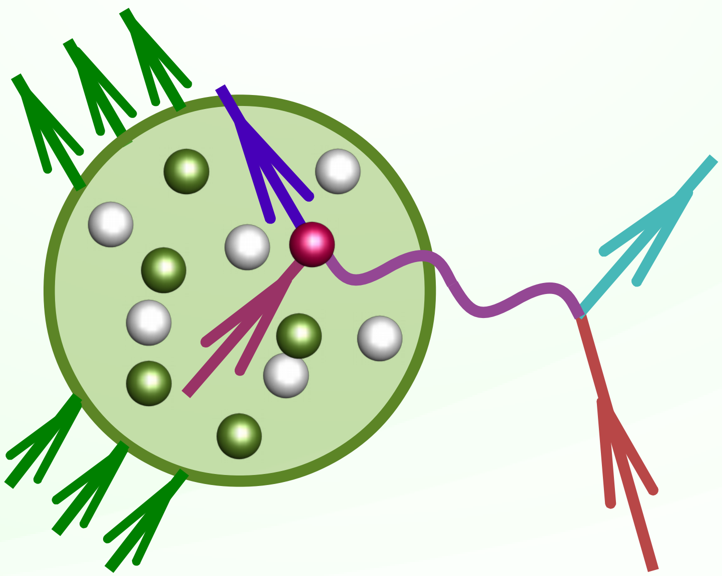

Importance of relativistic kinematics

A.M.A. & O. Benhar, PRC 83, 054616 (2011)

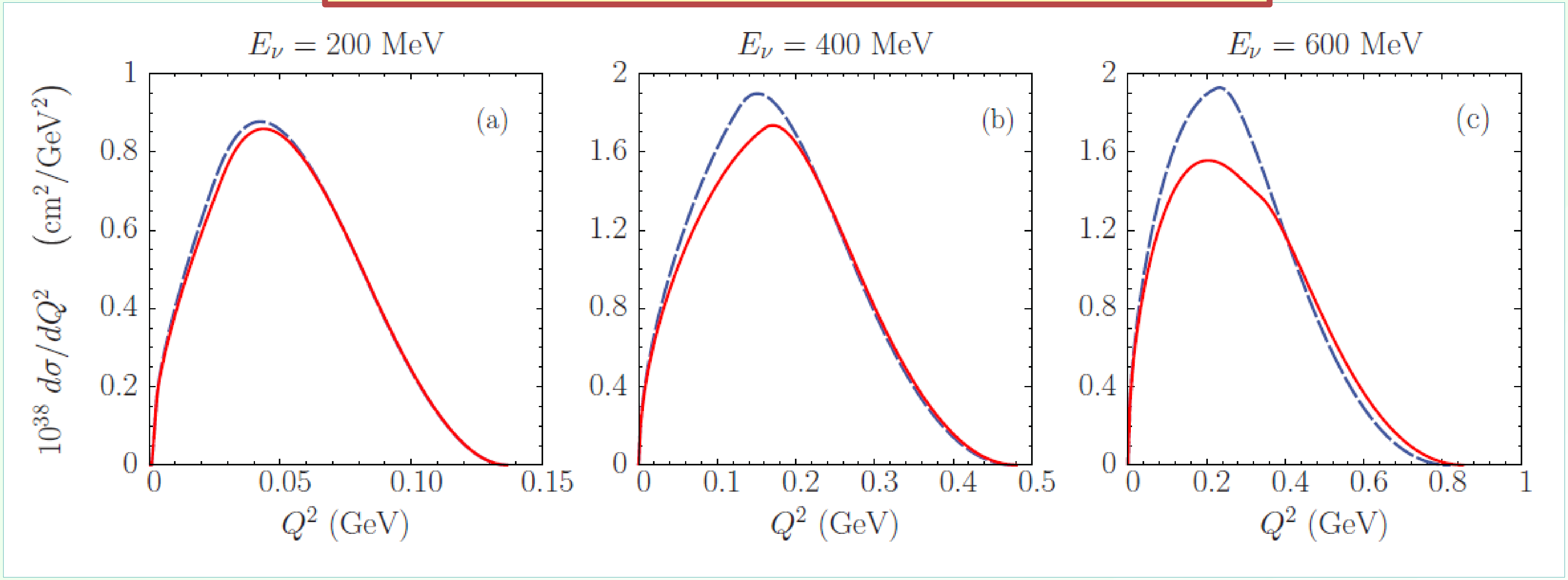

Sizable differences between the **relativistic** and **nonrelativistic** results at neutrino energies ~500 MeV.

Importance of relativistic kinematics

A.M.A. & O. Benhar, PRC 83, 054616 (2011)

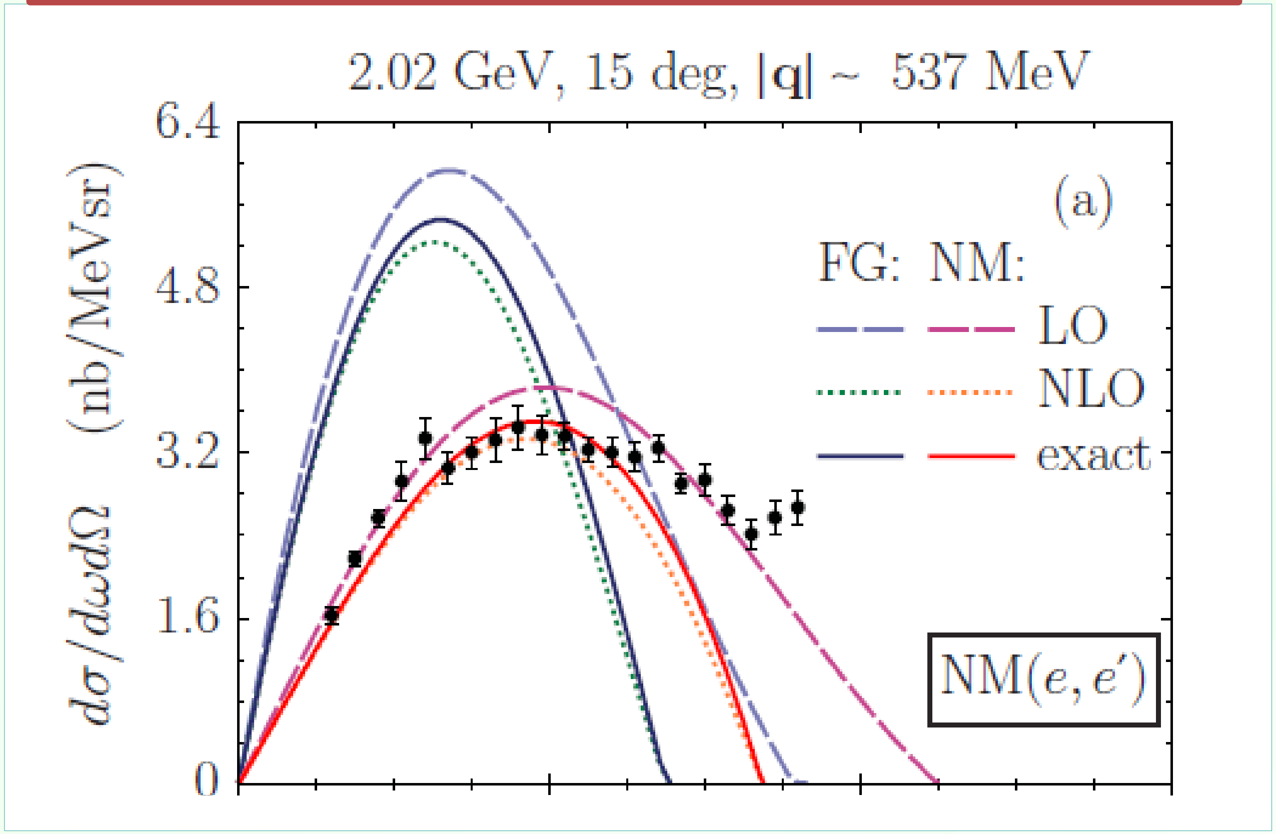

At |q|~540 MeV, semi-relativistic result is **5% lower** than the exact cross section.

Impulse approximation

For scattering in a given angle, neutrinos and electrons differ only due to **the elementary cross section**.

In neutrino scattering, uncertainties come from (i) interaction dynamics and (ii) **nuclear effects.**

It is **highly improbable** that theoretical approaches unable to reproduce *(e,e')* data would describe nuclear effects in neutrino interactions at similar kinematics.

Much more than the vector part...

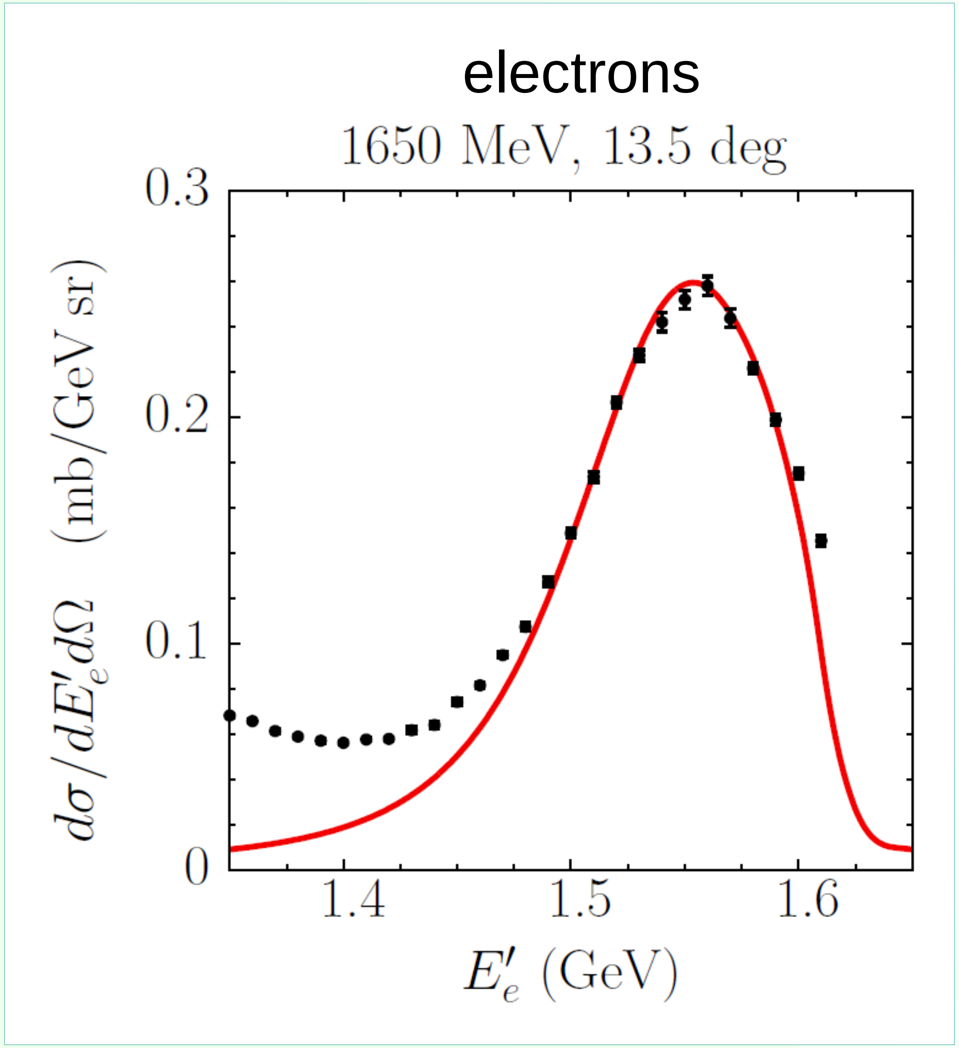

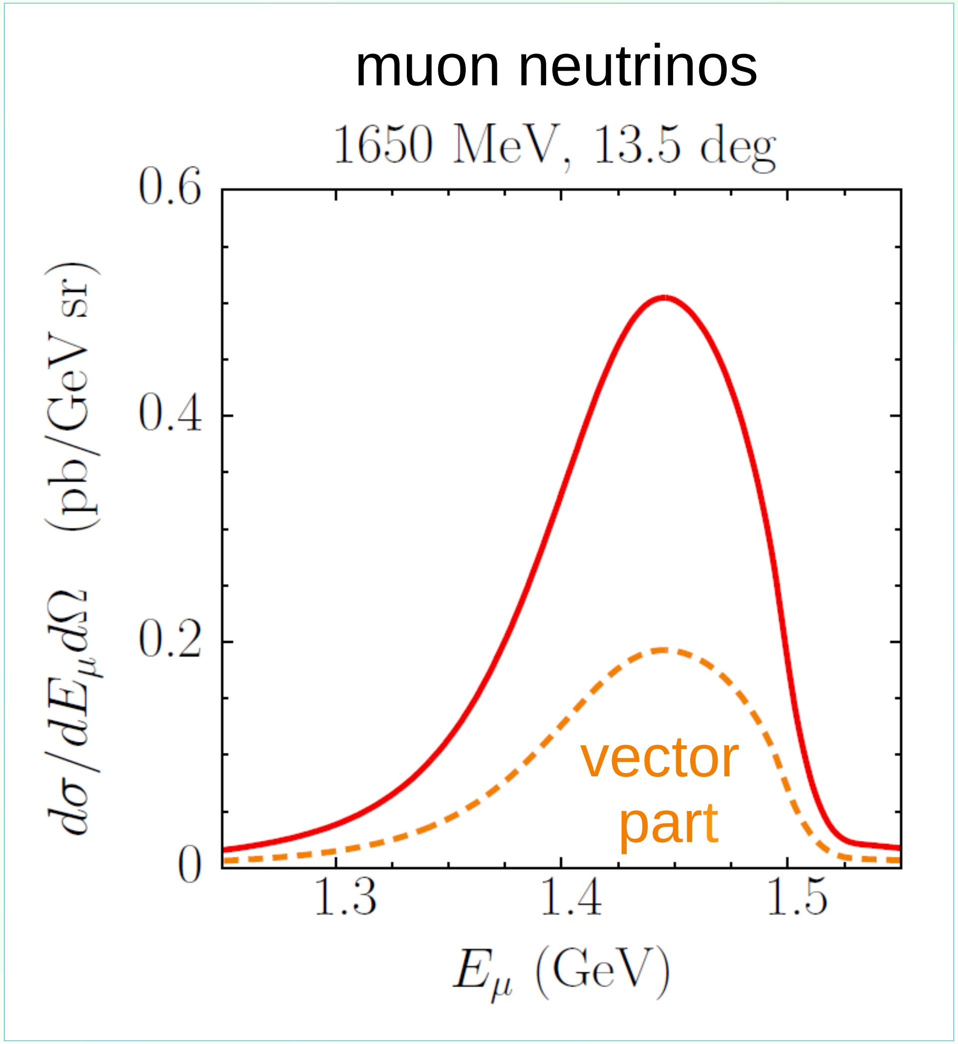

Fermi gas model

Fermi gas model

Imagine an infinite space filled uniformly with nucleons

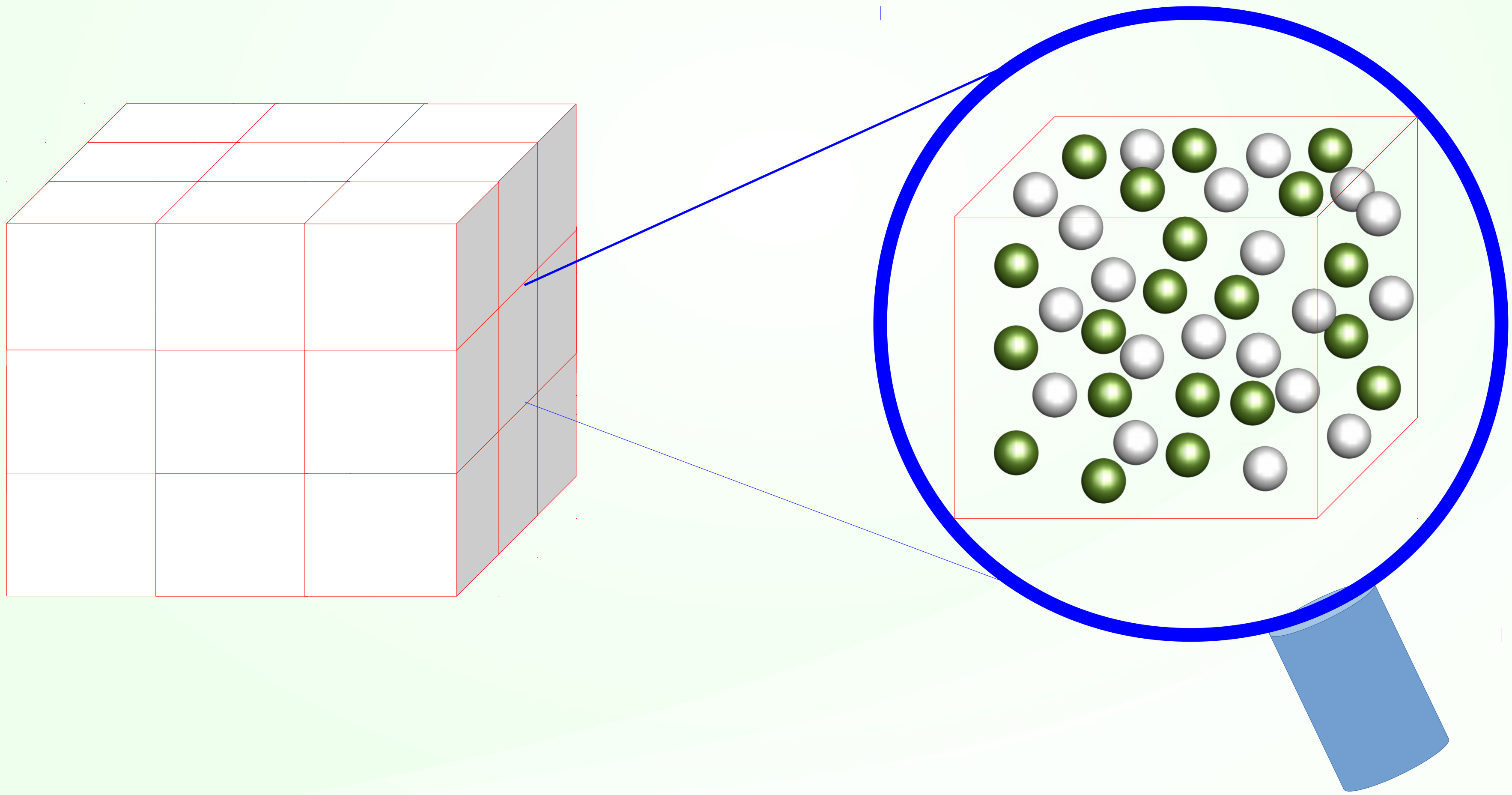

Fermi gas model

Due to the translational invariance, the eigenstates can be labeled using momentum, $\psi(x) = C e^{-i\boldsymbol{p}\boldsymbol{x}}$.

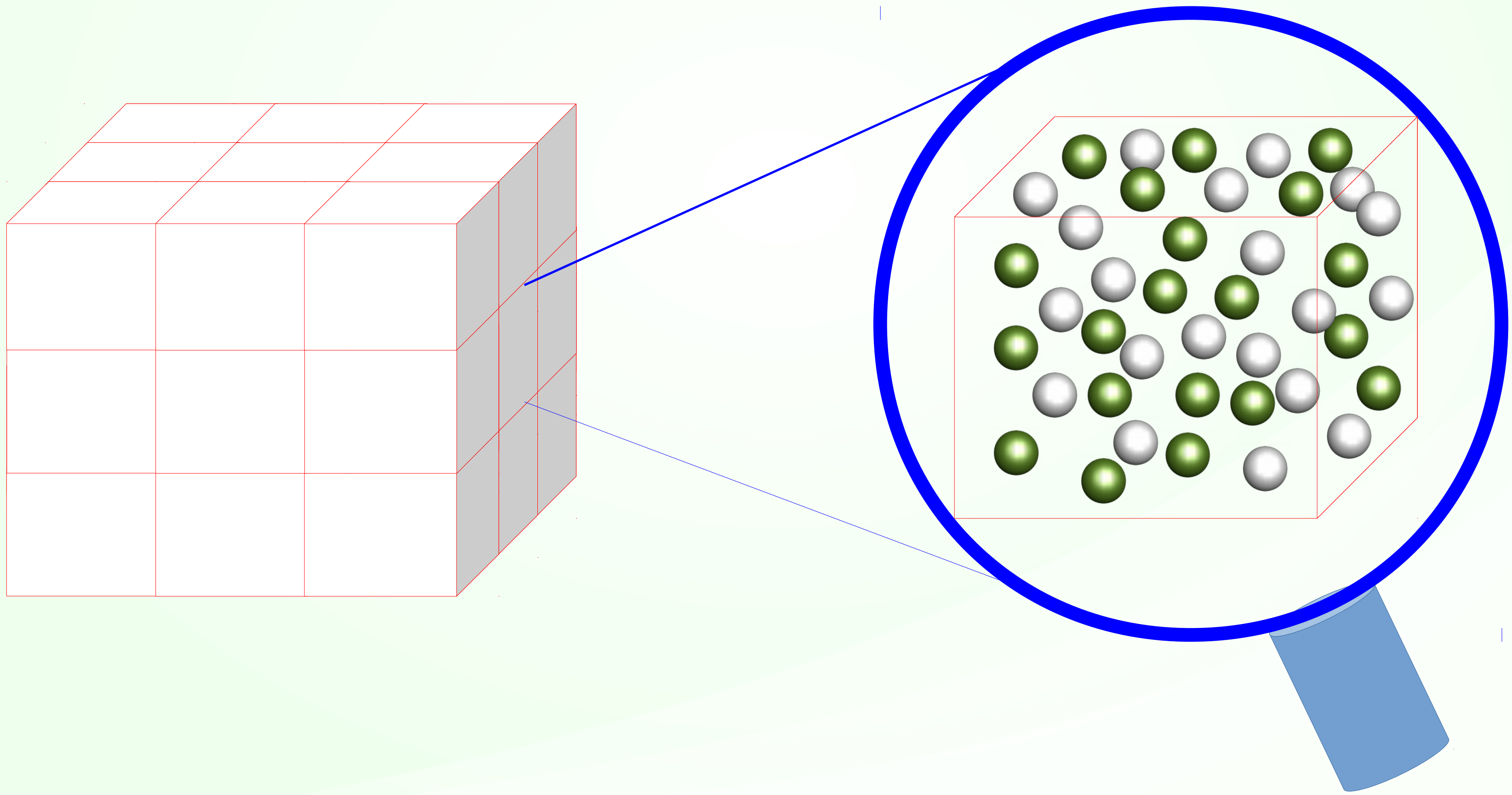

Fermi gas model

Due to the boundary conditions, $p_i \frac{L}{2} = \frac{\pi}{2} + n\pi$

every state occupies $(2\pi/L)^3$ in the momentum space

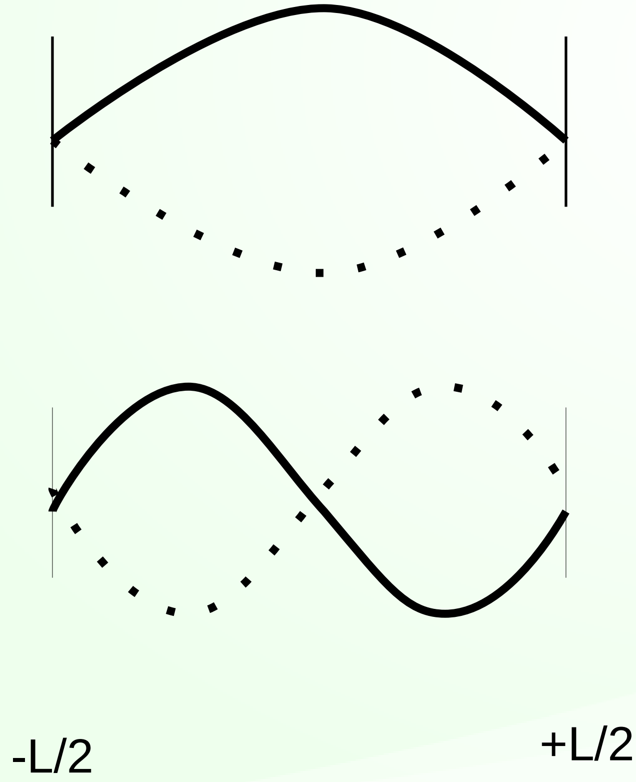

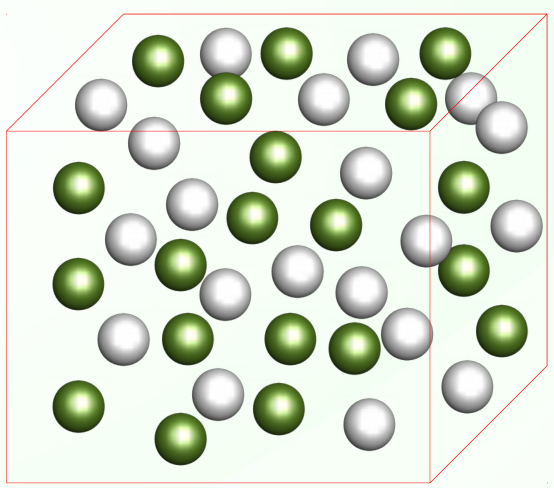

Fermi gas model

Due to the boundary conditions, $p_i \frac{L}{2} = \frac{\pi}{2} + n\pi$

every state occupies $(2\pi/L)^3$ in the momentum space

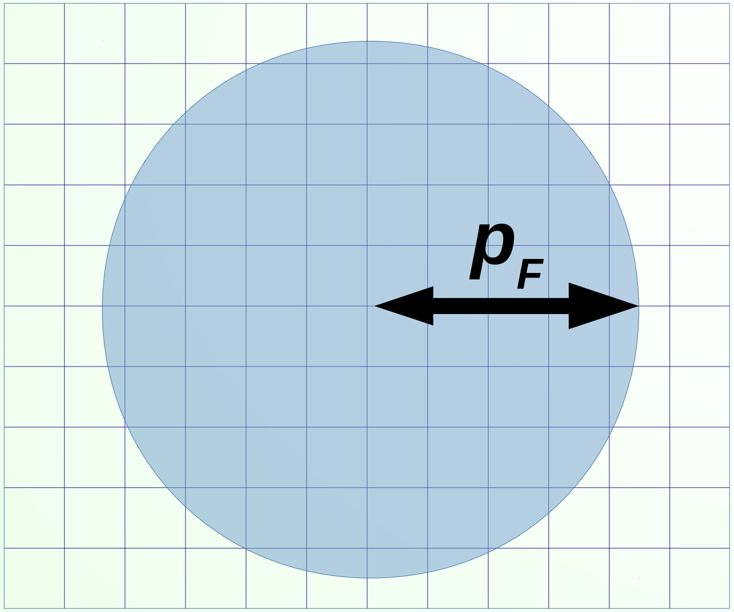

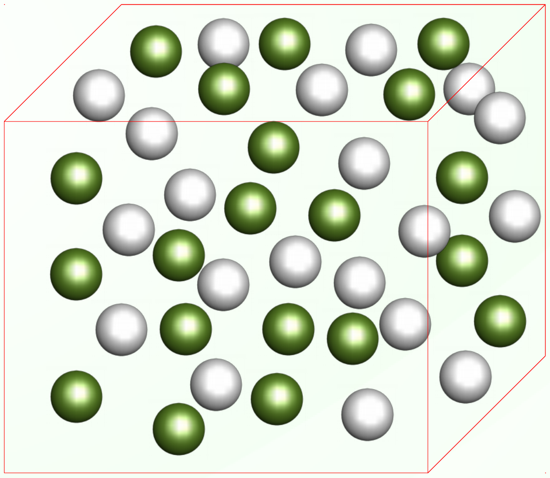

Momentum space

Coordinate space

Electron scattering off carbon, 500 MeV, 60 deg

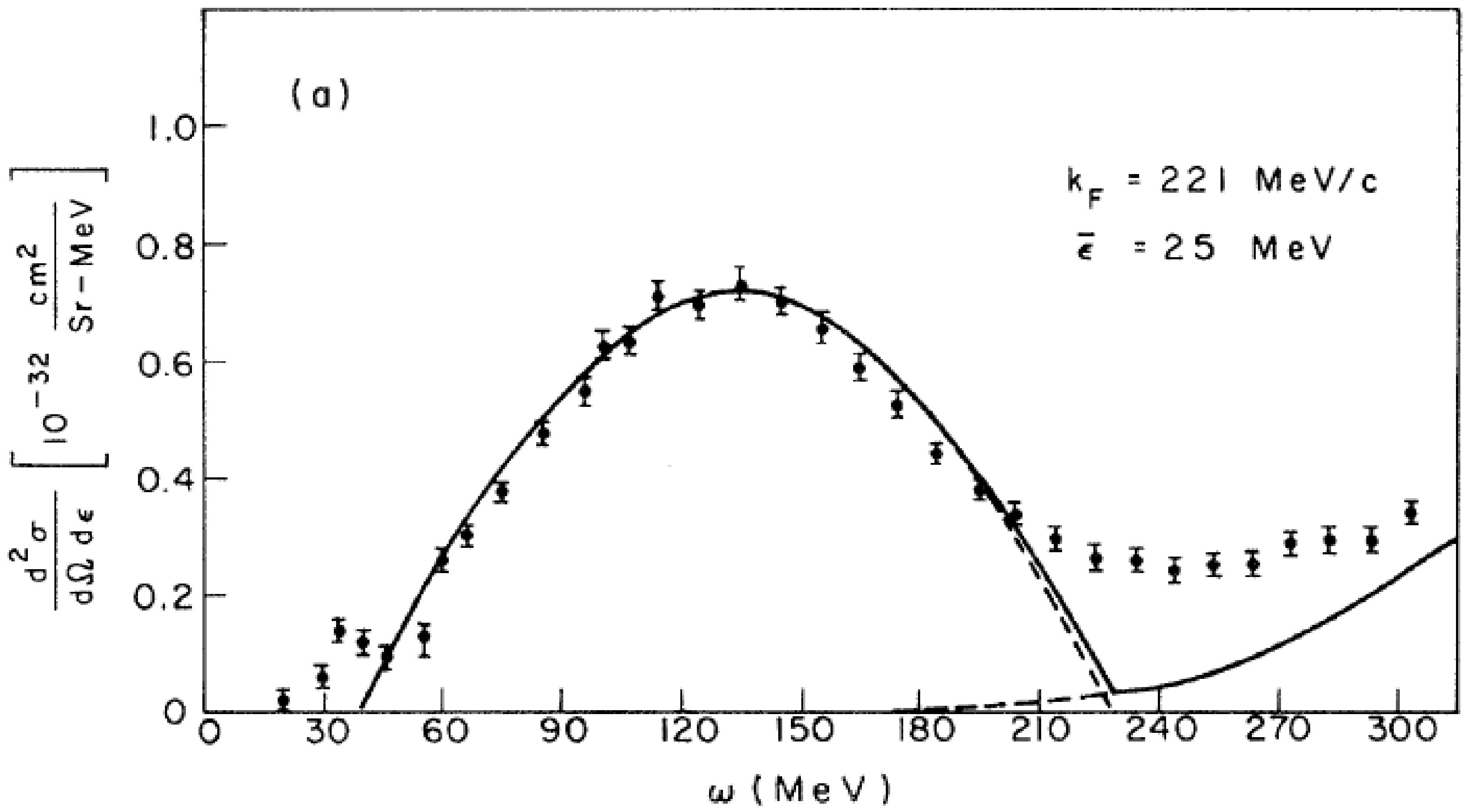

Moniz *et al.*, PRL 26, 445 (1971)

Electron scattering off carbon, 500 MeV, 60 deg

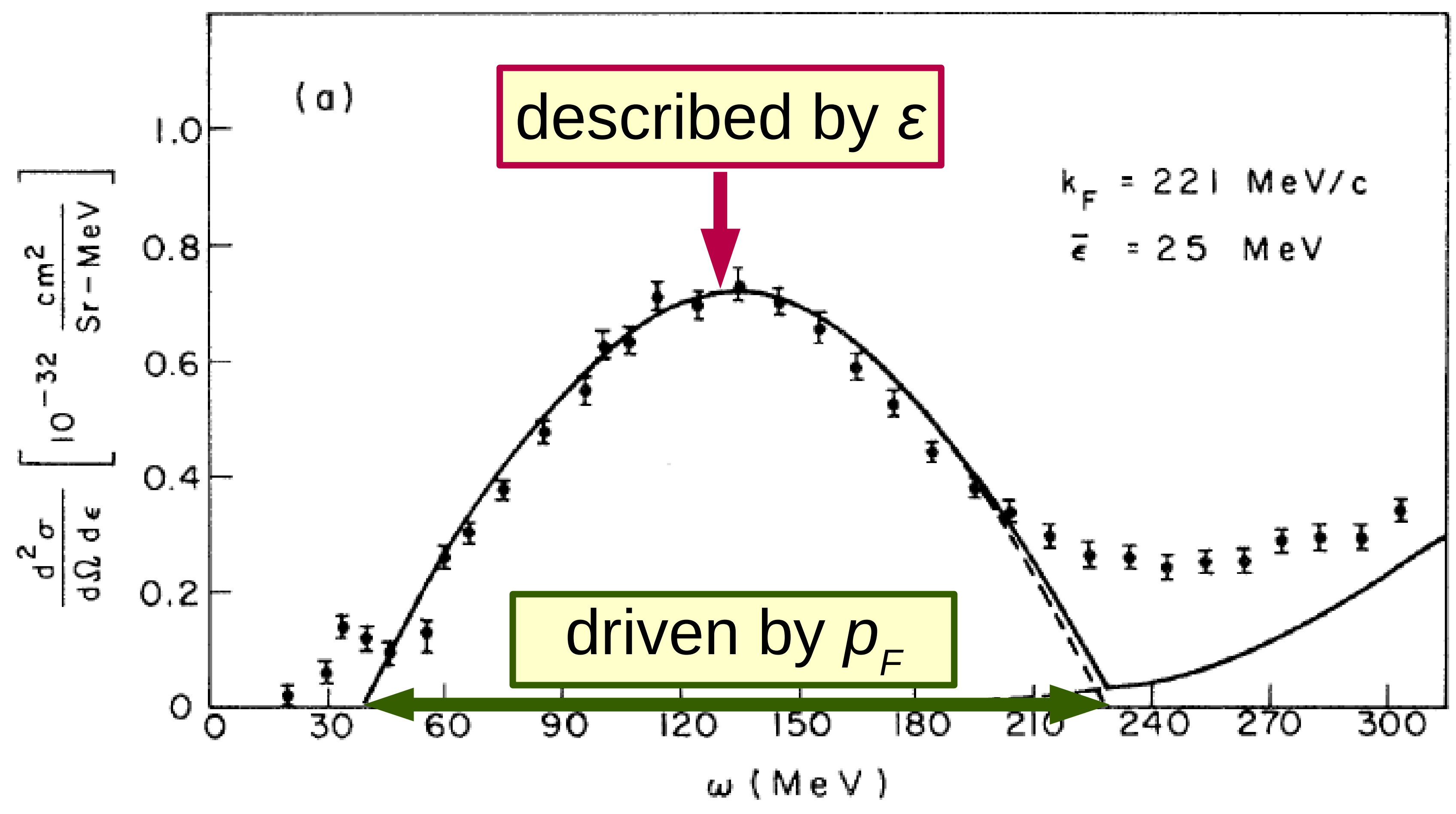

Moniz *et al.*, PRL 26, 445 (1971)

Fermi gas model

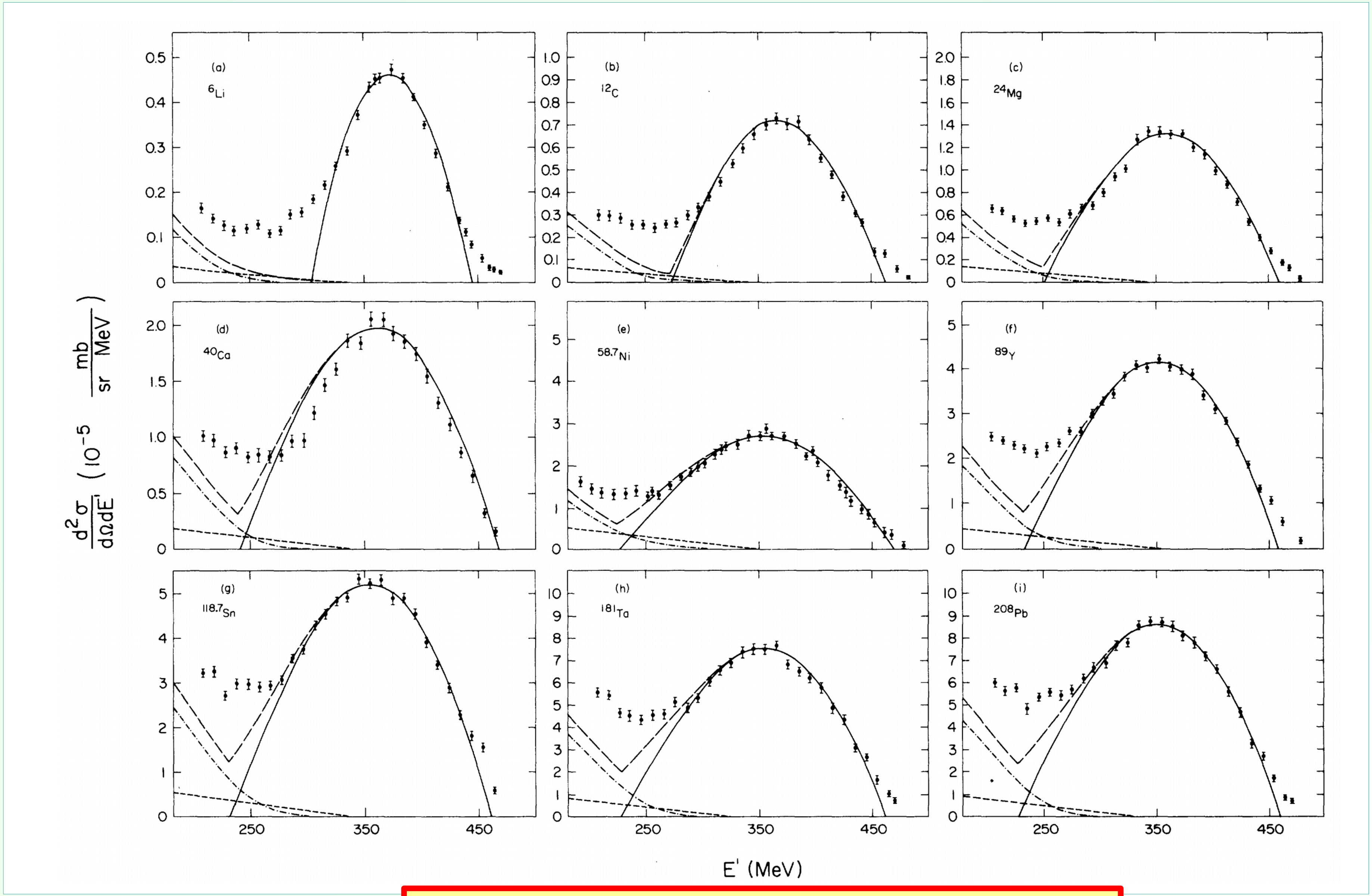

Whitney *et al.*, PRC 9, 2230 (1974)

Fermi gas model

What happens at kinematics other than 500 MeV, 60 deg?

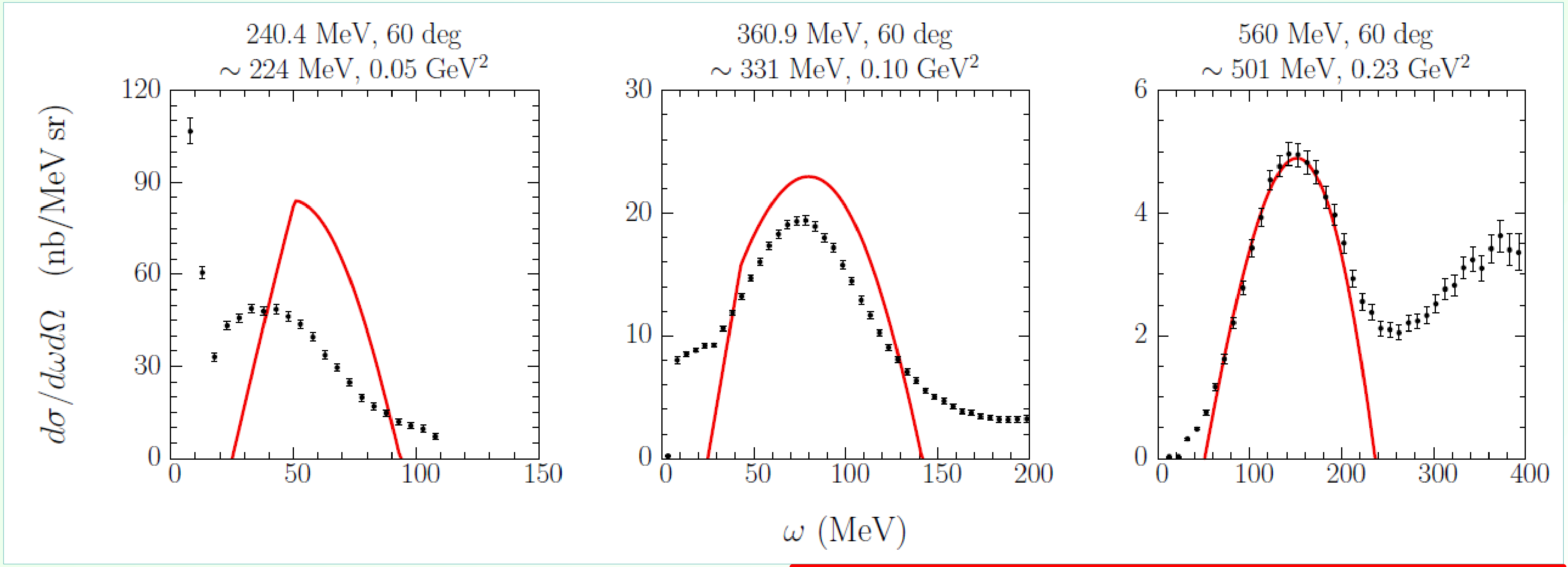

Barreau *et al.*, NPA 402, 515 (1983)

Charge-density in nuclei

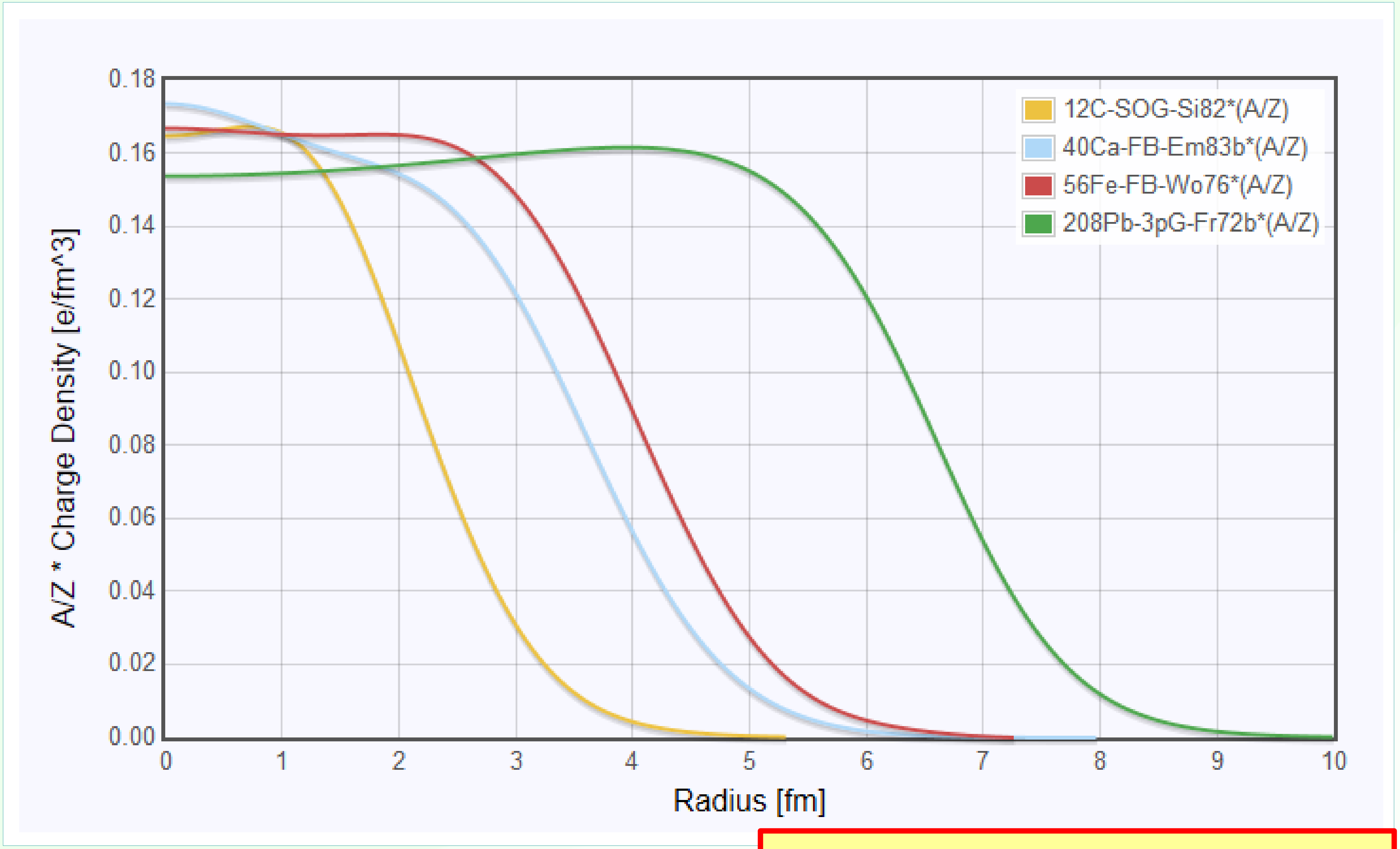

http://faculty.virginia.edu/ncd/index.htm

Local Fermi gas model

A spherically symmetric nucleus can be approximated by concentric spheres of a constant density.

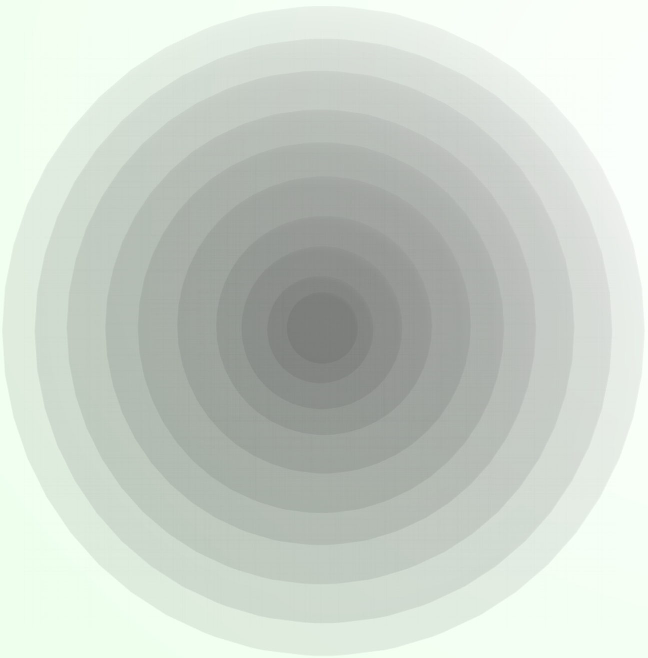

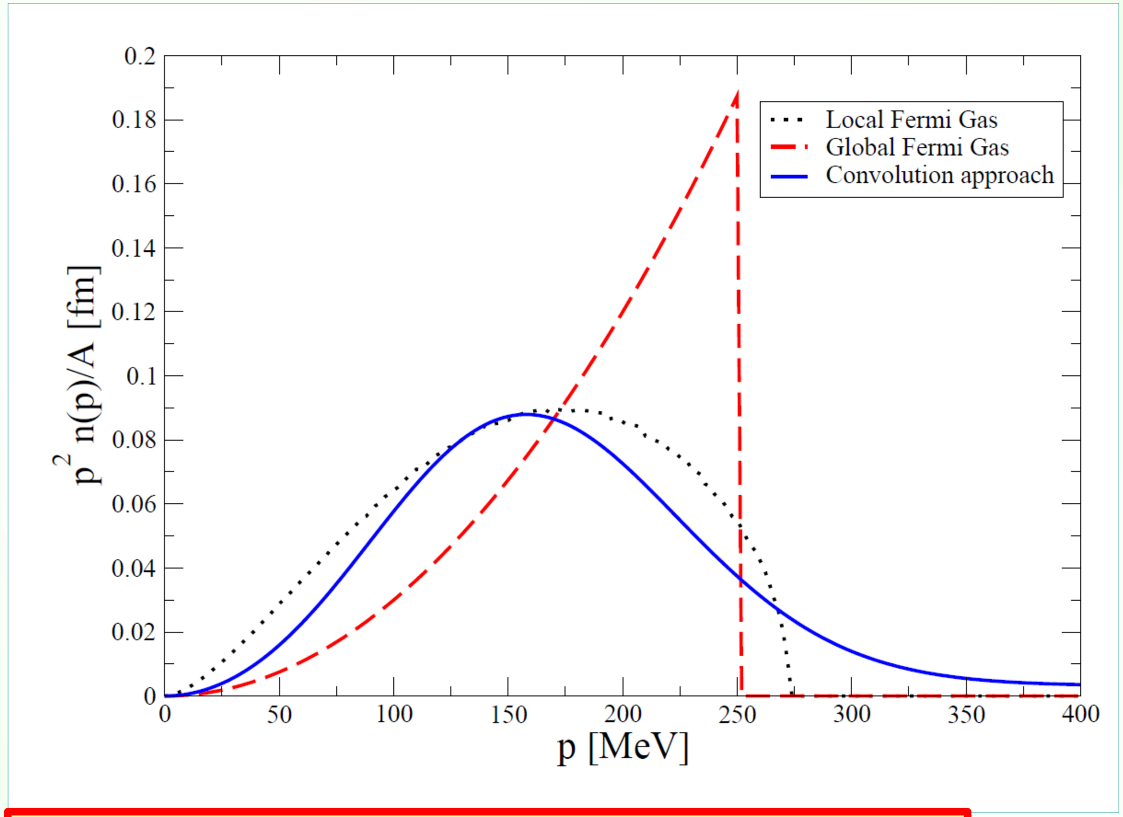

L. Alvarez-Ruso *et al.*,
New J.Phys. 16, 075015 (2014)

Local vs. global Fermi gas models

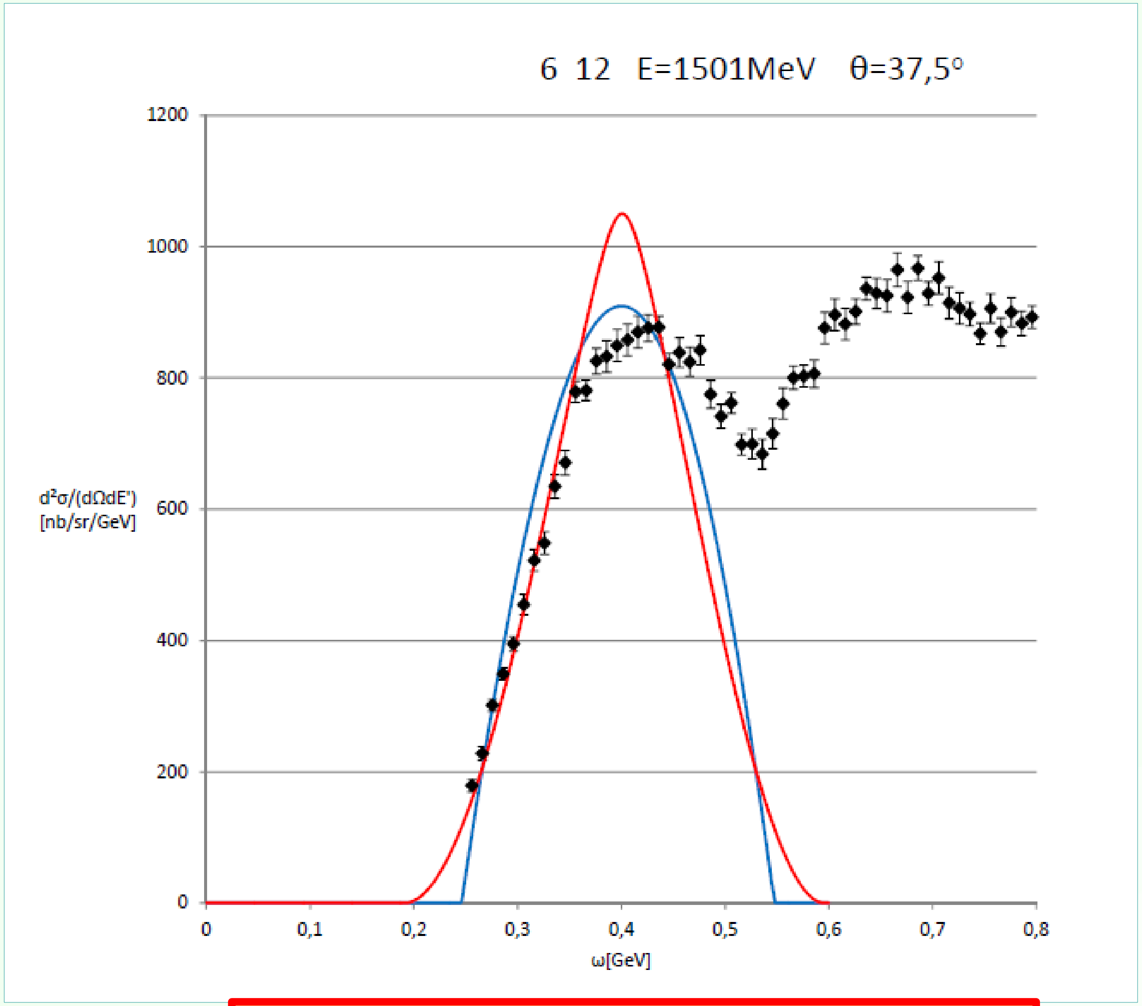

B. Kowal, M.Sc. thesis, University of Wroclaw (2014)

Shell model

Shell model

In a spherically symmetric potential, the eigenstates can be labeled using the total angular momentum.

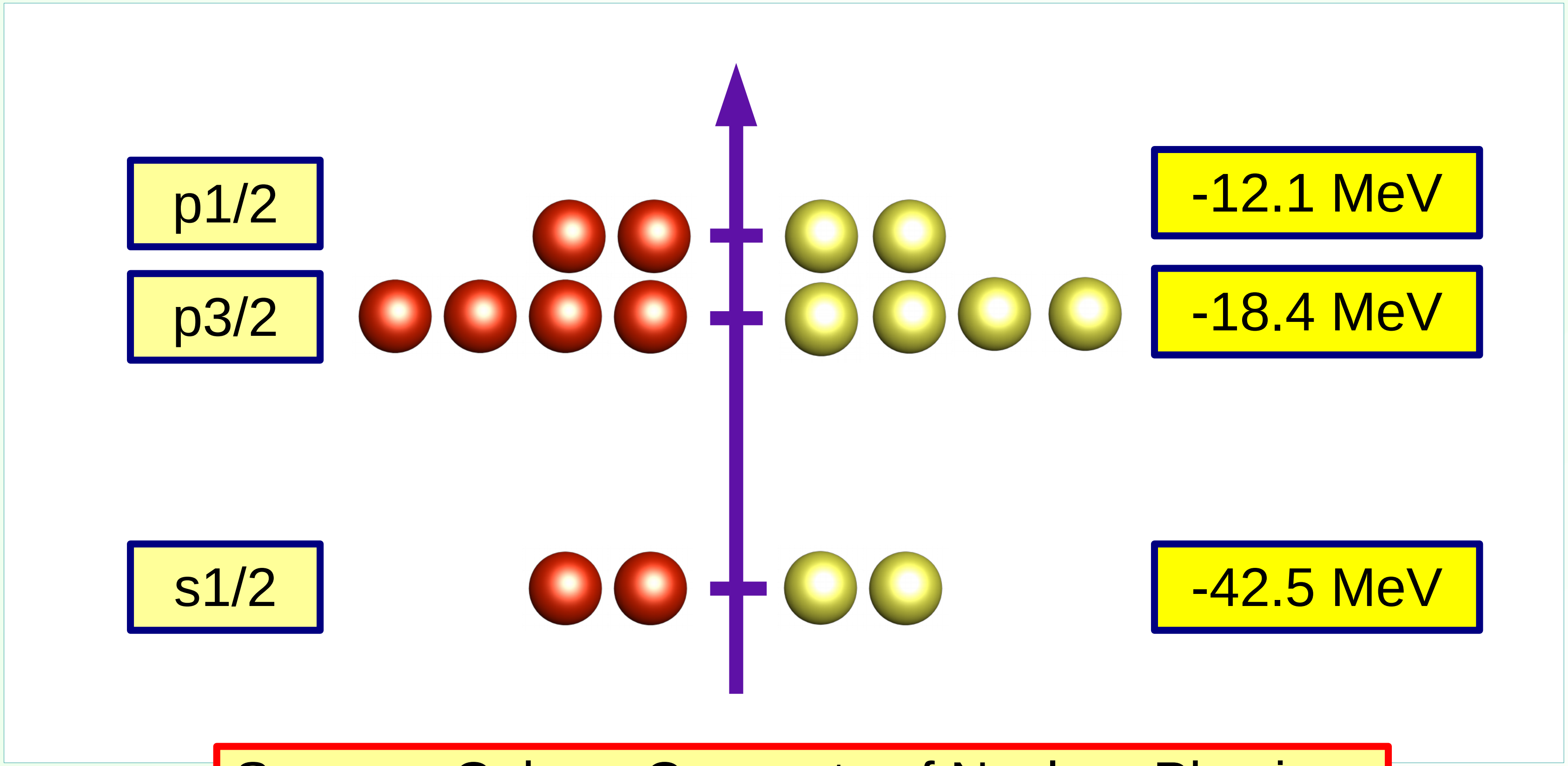

See e.g. Cohen, Concepts of Nuclear Physics, McGraw-Hill, 1971

Example: oxygen nucleus

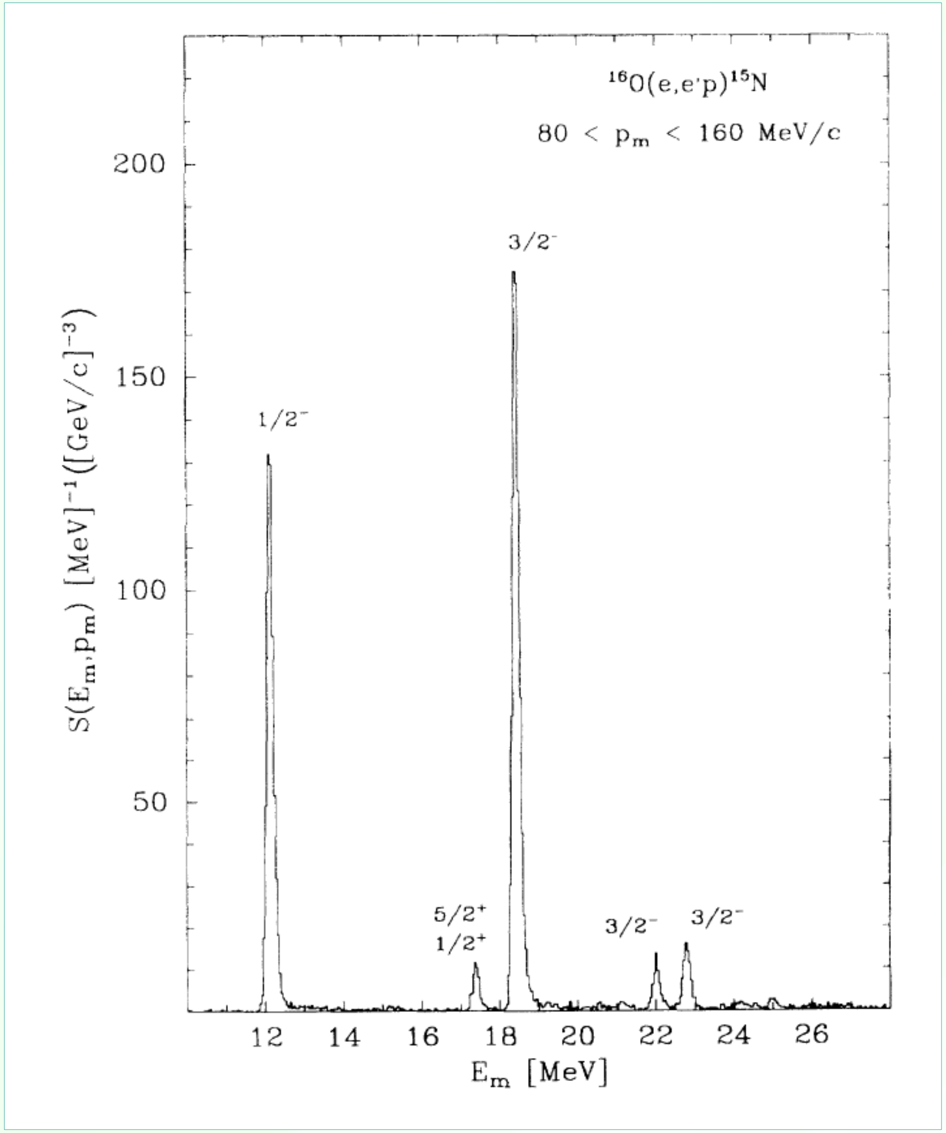

Leuschner *et al.*, PRC 49, 955 (1994)

Example: oxygen spectral function

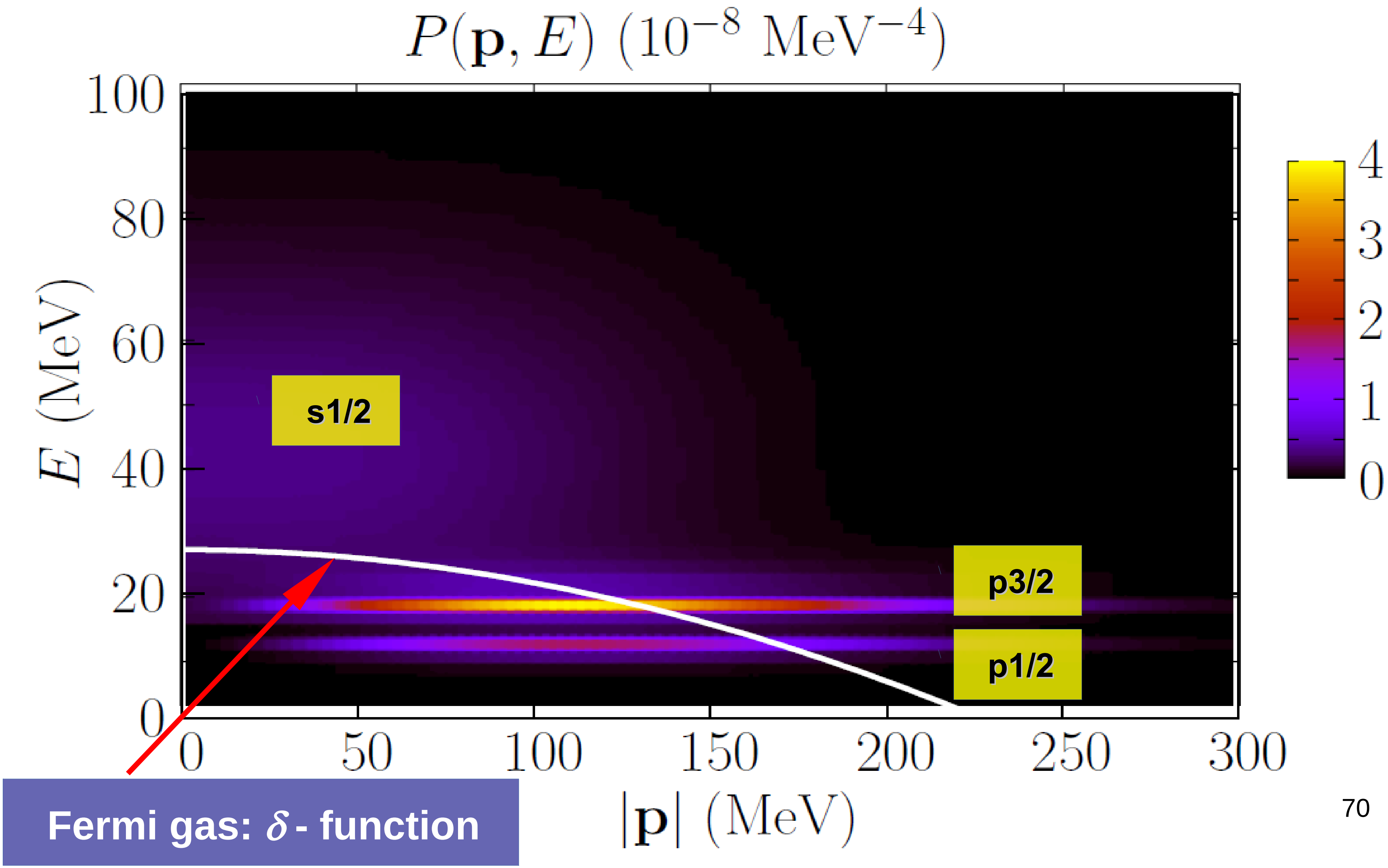

Depletion of the shell-model states

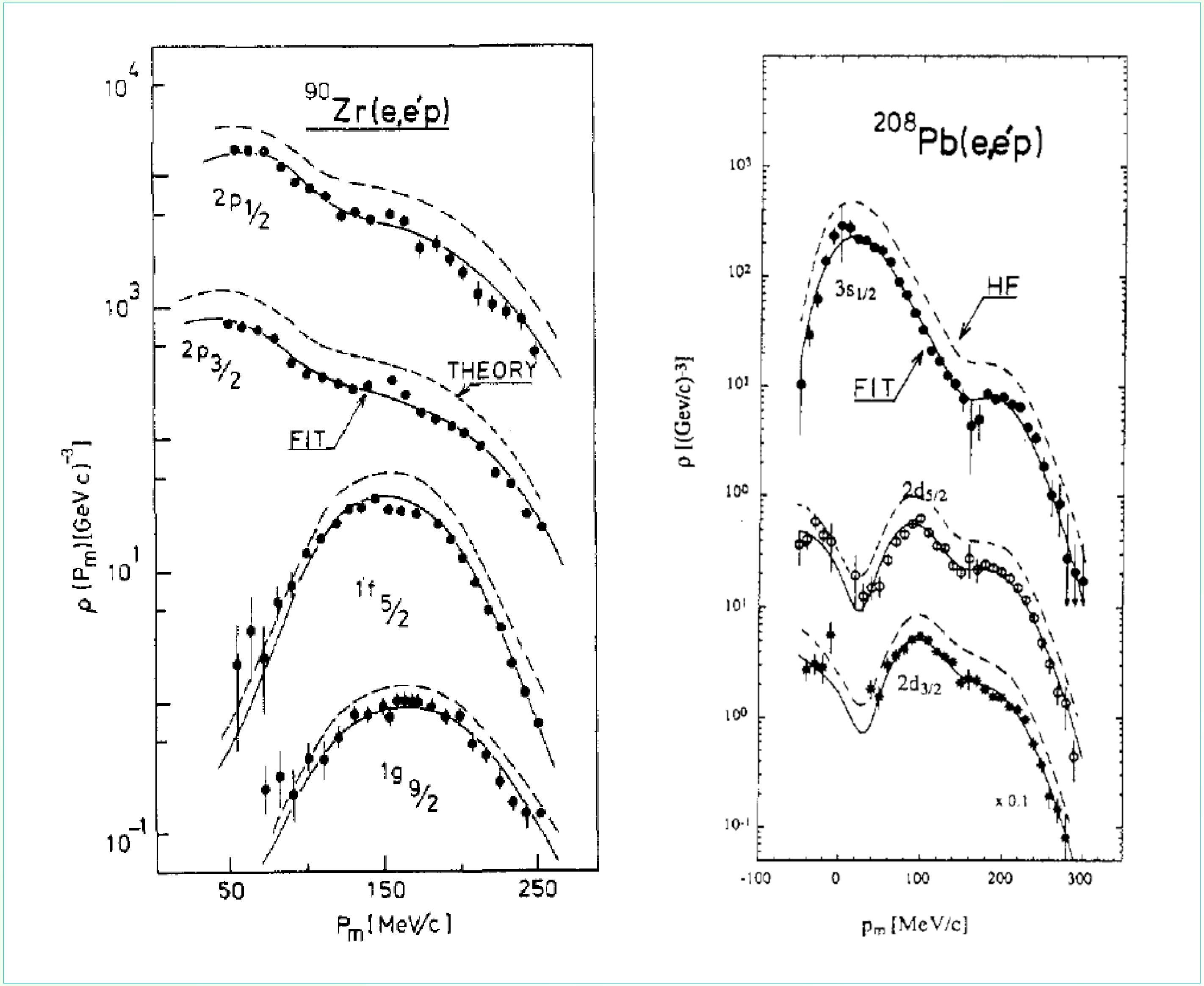

De Witt Huberts, JPG 16, 507 (1990)

Depletion of the shell-model states

The observed depletion is ~35% for the valence shells (LRC and SRC) and ~20% when higher missing energy is probed (SRC).

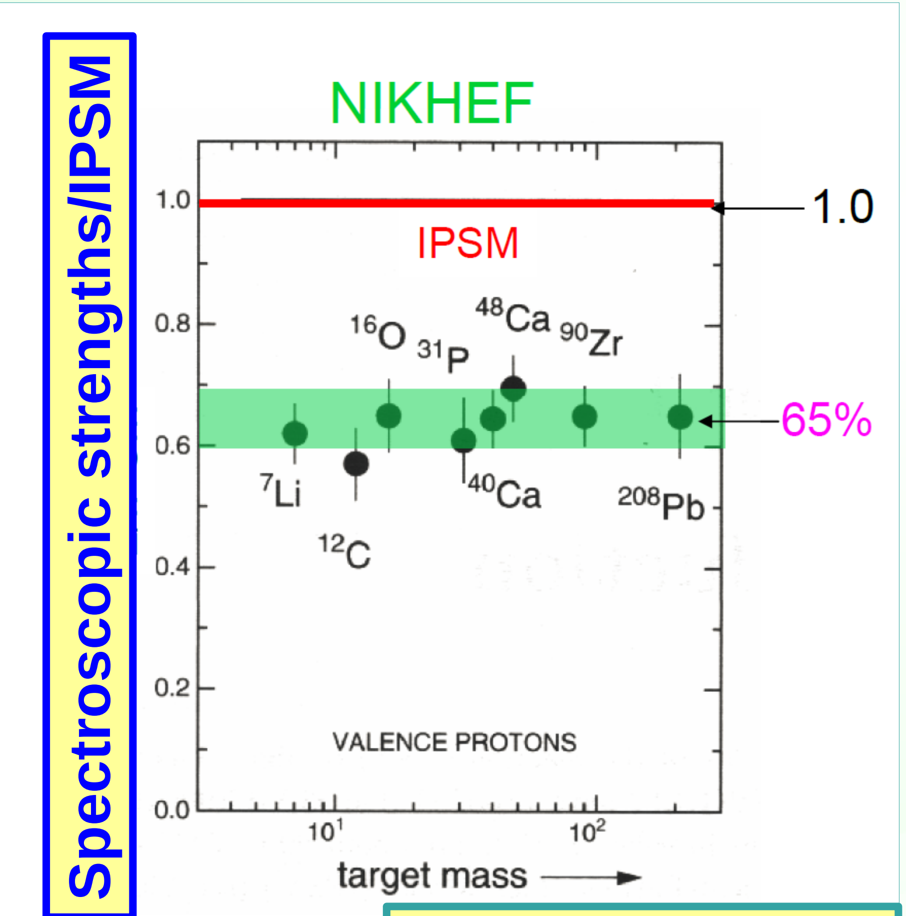

D. Rohe, NuInt05

NIKHEF: ^{208}Pb(e,e'p)^{207}Tl

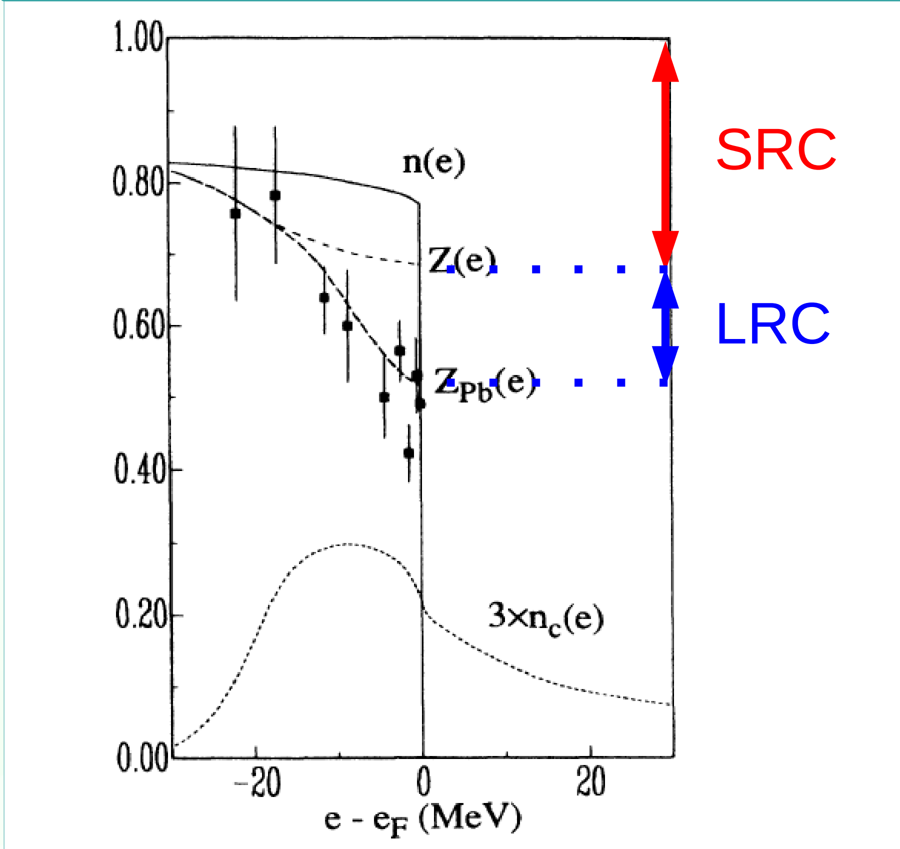

Benhar et al, PRC 41, R24 (1990)

Spectral function approach

Short-range correlations

The main source of the depletion of the shell-model states at high *E* are **short-range nucleon-nucleon correlations**.

Yielding NN pairs (typically pn pairs) with high relative momentum, they move ~20% of nucleons to the states of high removal energies.

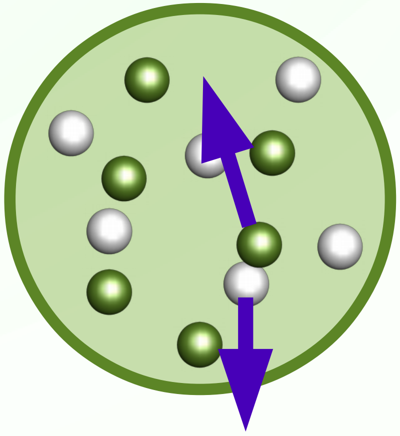

Short-range correlations

The hole spectral function can be expressed as

$$P_N(\mathbf{p}, E) = \sum_\alpha \underline{n_\alpha |\phi_\alpha|^2 f_\alpha(E - E_\alpha^N)} + \underline{P_{\mathrm{corr}}^N(\mathbf{p}, E)},$$

describes the contribution of the shell-model states, vanishes at high |p| or high *E*

relevant only at high |p| **and** *E*

Short-range correlations

Momentum distributions

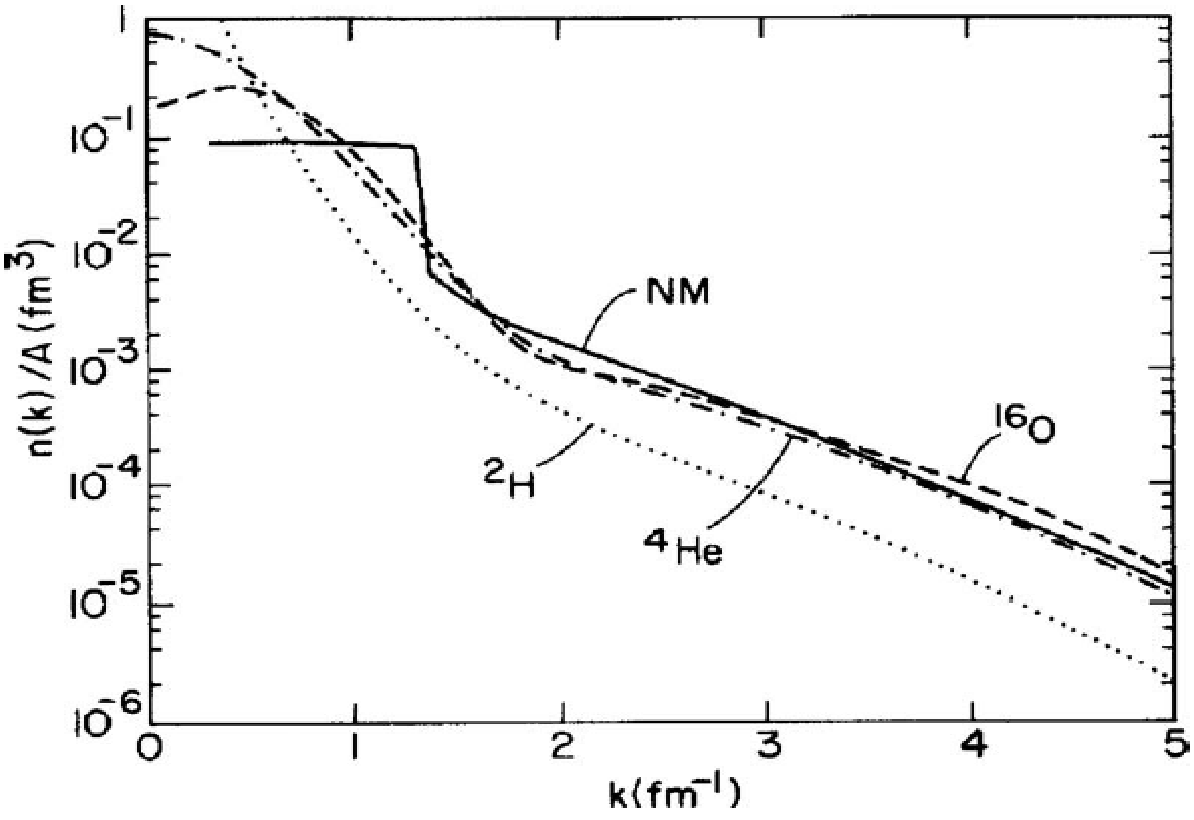

Benhar&Pandharipande, RMP 65, 817 (1993)

Short-range correlations

Momentum distributions

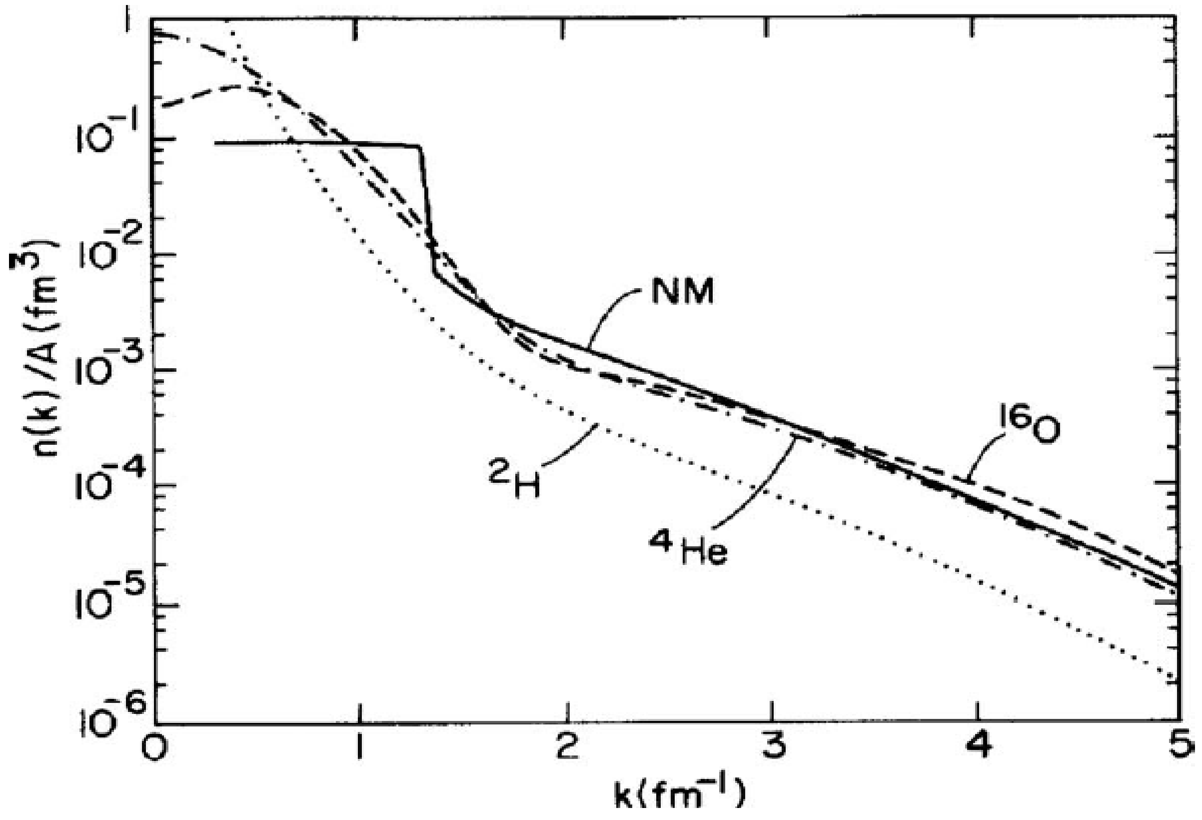

SRC don't depend on the shell structure or finite-size effects, only on the density

Local-density approximation

The correlation component in nuclei can be obtained combining the results for infinite nuclear matter obtained at different densities:

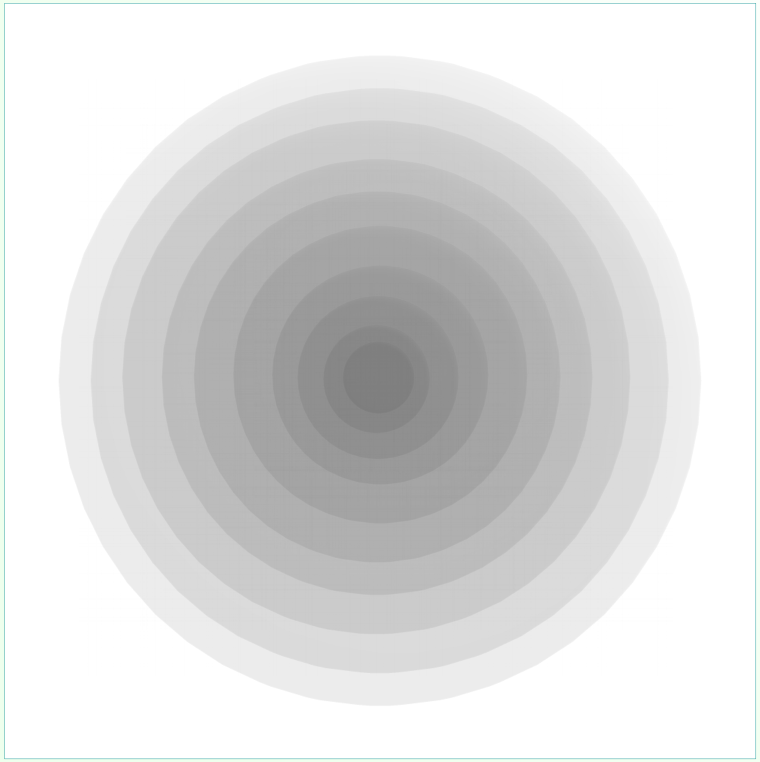

$$P^{N}_{\rm corr}(\mathbf{p}, E) = \int dR\, \rho(R) P^{NM,N}_{\rm corr}(\rho, \mathbf{p}, E).$$

Benhar *et al.*, NPA 579 493, (1994), included Urbana v_{14} NN interactions and 3N interactions [Lagaris & Pandharipande]

FSI in the spectral function approach

Artur M. Ankowski
SLAC, Stanford University

A.M.A, O. Benhar and M. Sakuda,
Phys. Rev. D 91, 033005 (2015)

Testing and Improving Models
of Neutrino-Nucleus Interactions in Generators
ECT*, Trento, June 3−7, 2019

Comparison to C(*e*, *e*′) data

13.5°

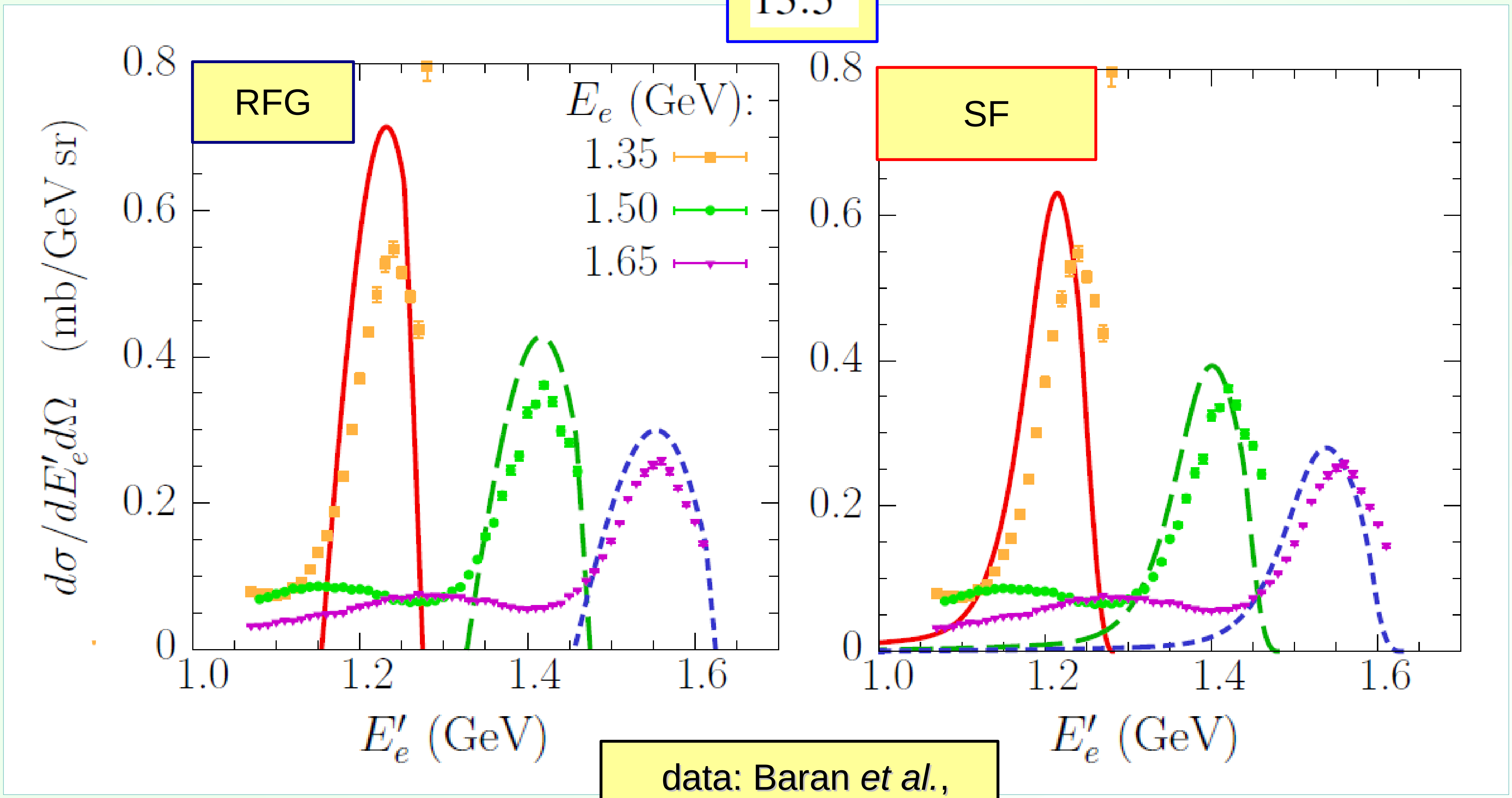

data: Baran *et al.*,
PRL 61, 400 (1988)

Energy conservation

$$E_{\mathbf{k}} + M_A = E_{\mathbf{k}'} + E_{A-1} + E_{\mathbf{p}'}$$

Energy conservation

$$E_{\mathbf{k}} + M_A = E_{\mathbf{k}'} + E_{A-1} + E_{\mathbf{p}'}$$

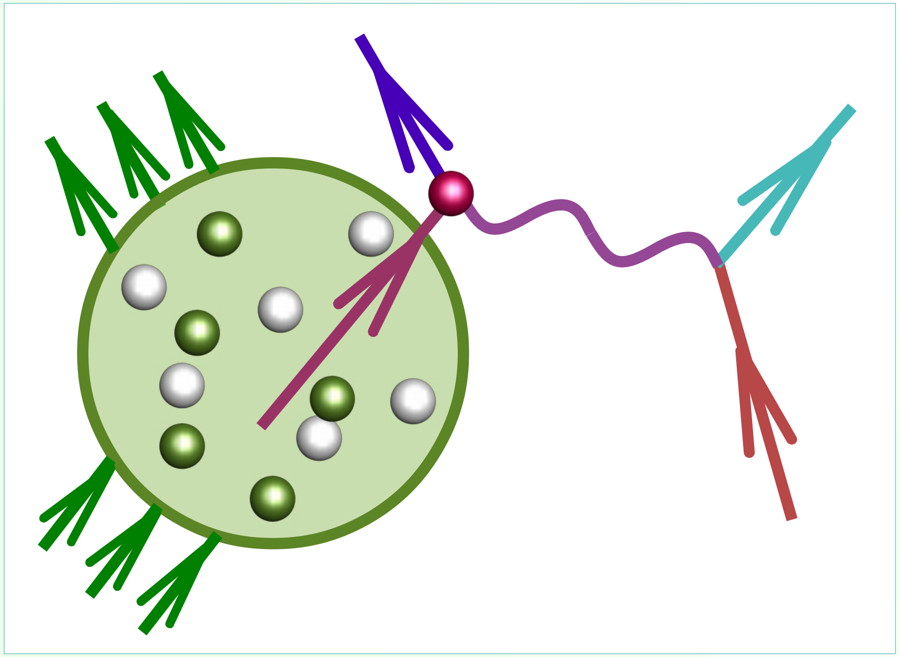

Energy conservation

$$E_{\mathbf{k}} + M_A = E_{\mathbf{k}'} + E_{A-1} + E_{\mathbf{p}'}$$

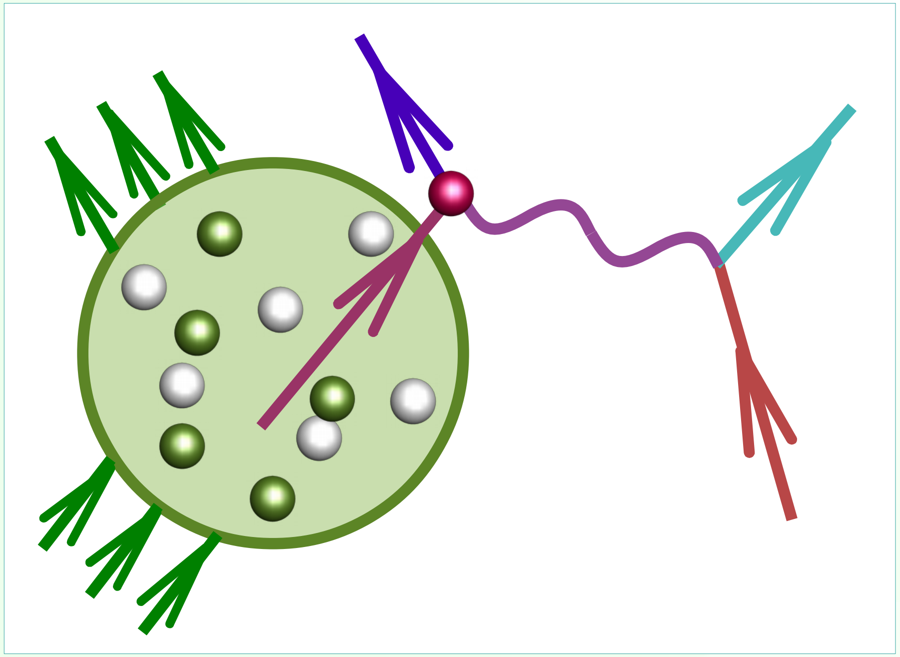

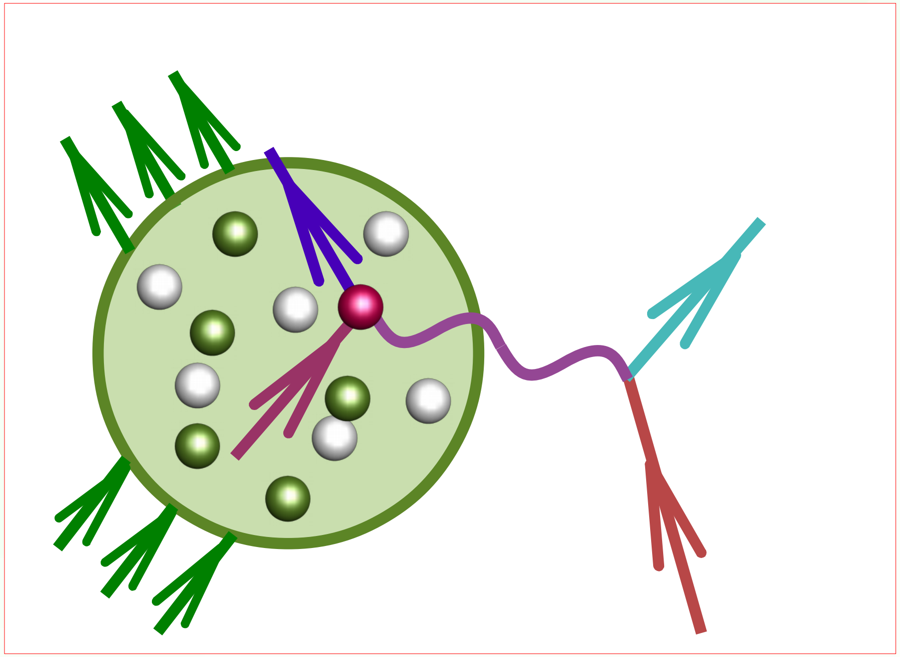

Energy conservation

$$E_{\mathbf{k}} + M_A = E_{\mathbf{k}'} + E_{A-1} + E_{\mathbf{p}'}$$

$$E_{\mathbf{k}} + M_A = E_{\mathbf{k}'} + E_{A-1} + E_{\mathbf{p}'} + U_V(\mathbf{p}')$$

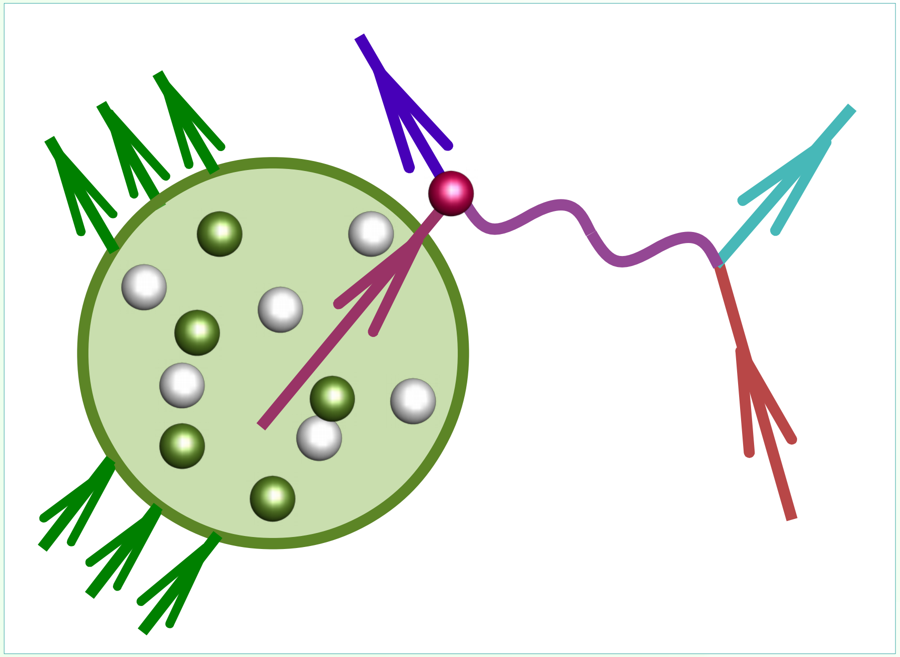

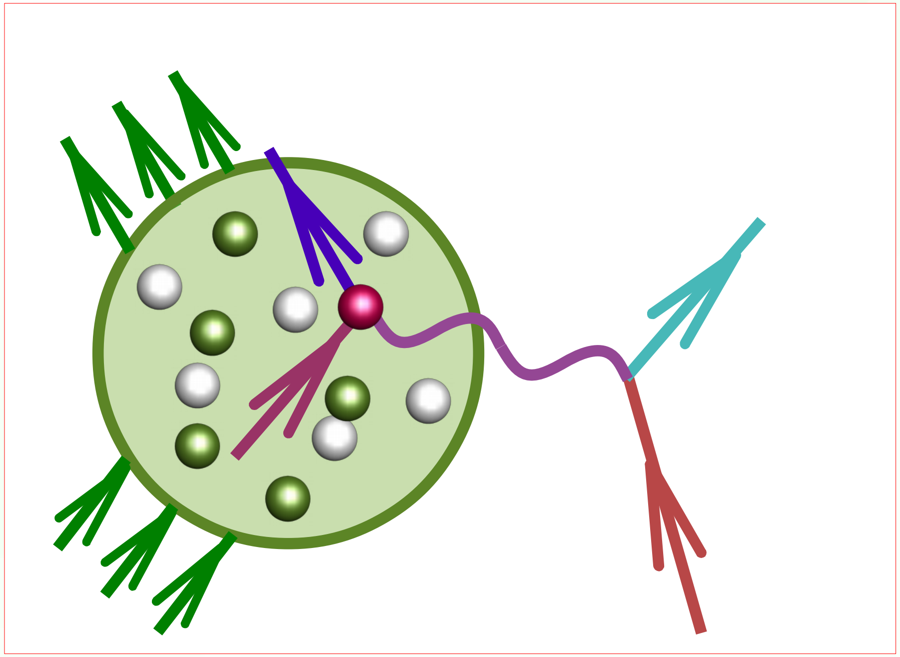

Energy conservation

$$E_{\mathbf{k}} + M_A = E_{\mathbf{k}'} + E_{A-1} + E_{\mathbf{p}'}$$

$$E_{\mathbf{k}} + M_A \boxed{\sim} E_{\mathbf{k}'} + E_{A-1} + E_{\mathbf{p}'} + U_V(\mathbf{p}')$$

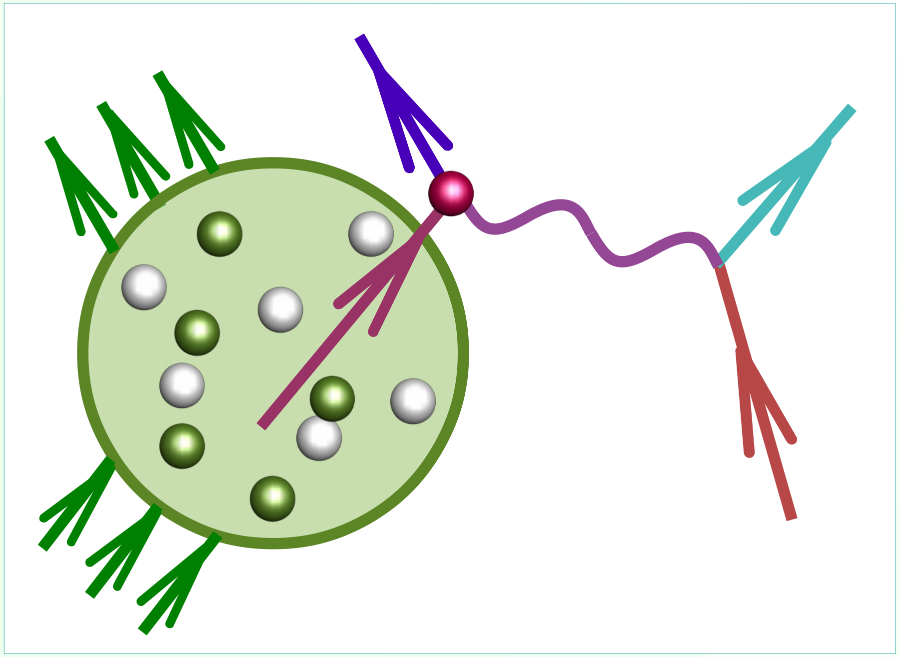

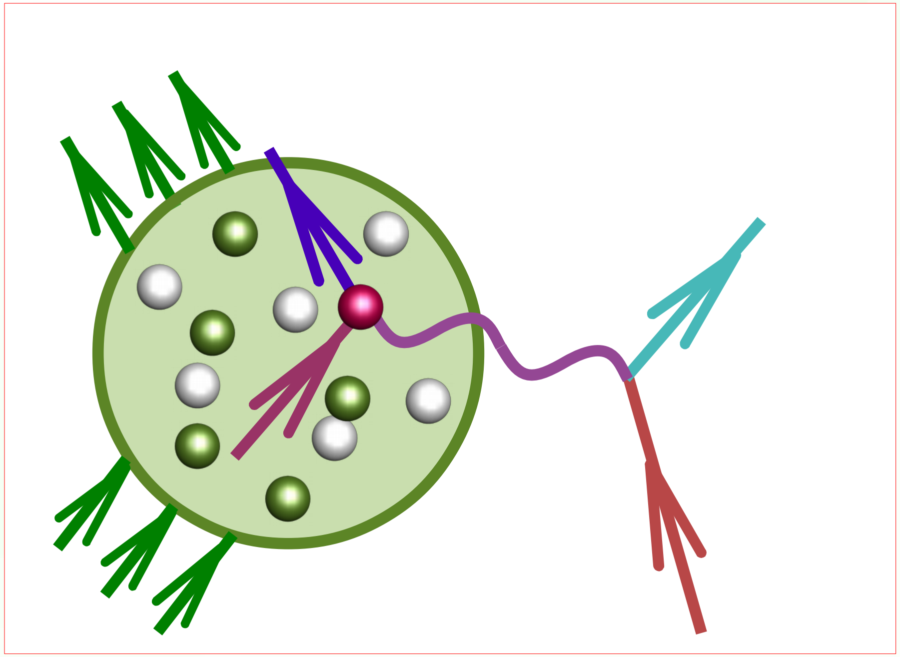

Final-state interactions

Their effect on the cross section is easy to understand in terms of the complex optical potential:

- the **real part** modifies the struck nucleon's energy spectrum: it differs from $\sqrt{M^2 + \mathbf{p}'^2}$
- the **imaginary part** reduces the single-nucleon final states and produces multinucleon final states

$$\boxed{e^{i(E+U)t} = e^{i(E+U_V)t} e^{-U_W t}}$$

Horikawa *et al.*, PRC 22, 1680 (1980)

Final-state interactions

In the convolution approach,

$$\boxed{\frac{d\sigma^{\mathrm{FSI}}}{d\omega d\Omega} = \int d\omega' f_{\mathbf{q}}(\omega - \omega') \frac{d\sigma^{\mathrm{IA}}}{d\omega' d\Omega},}$$

with the folding function

$$\boxed{f_{\mathbf{q}}(\omega) = \delta(\omega)\sqrt{T_A} + \left(1 - \sqrt{T_A}\right) F_{\mathbf{q}}(\omega),}$$

Nucl. transparency

Nuclear transparency

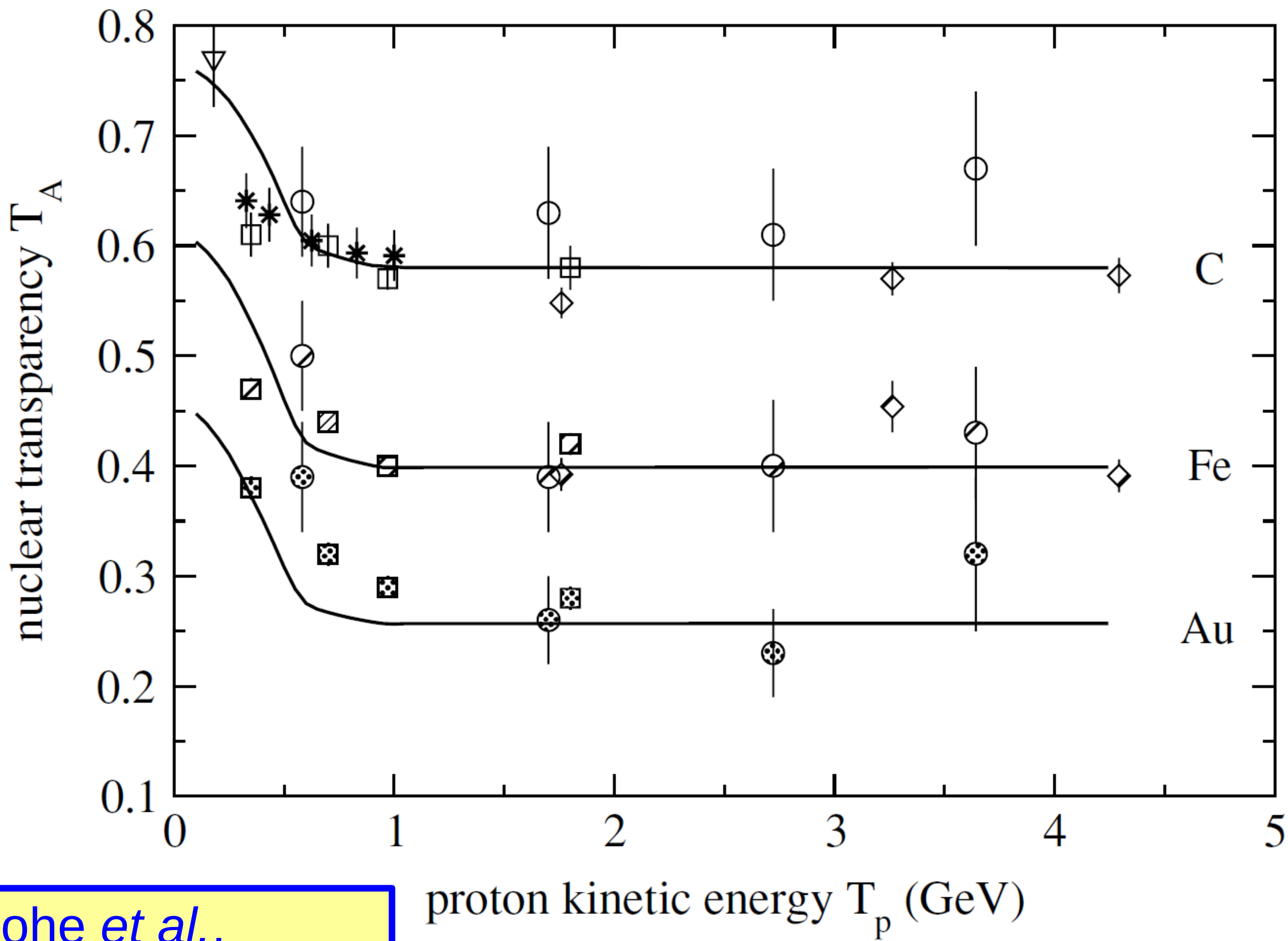

Rohe *et al.*,
PRC 72, 054602 (2005)

Nuclear transparency

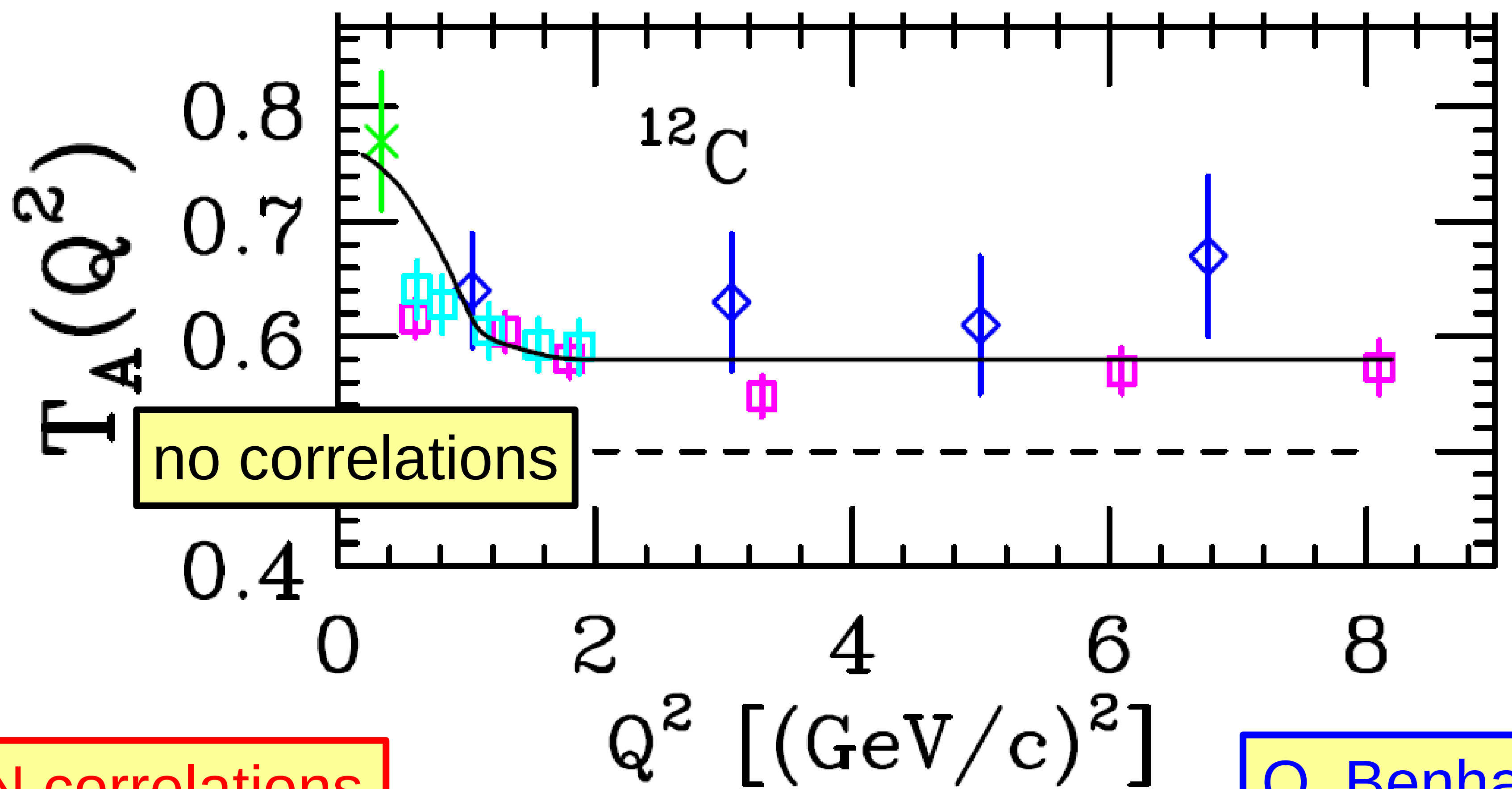

NN correlations
reduce FSI

O. Benhar
@ NuInt05

Short-range correlations

Pair distribution function of NM

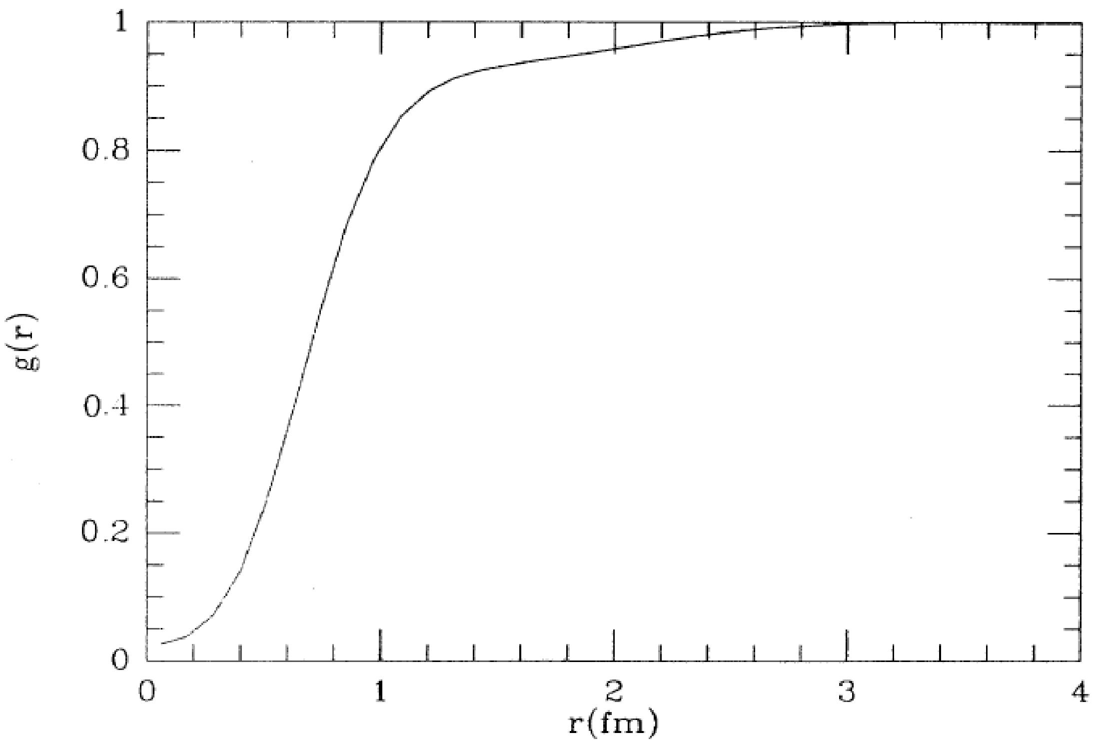

Benhar *et al.*, PRC 44, 2328 (1991)

$F_q(\omega)$

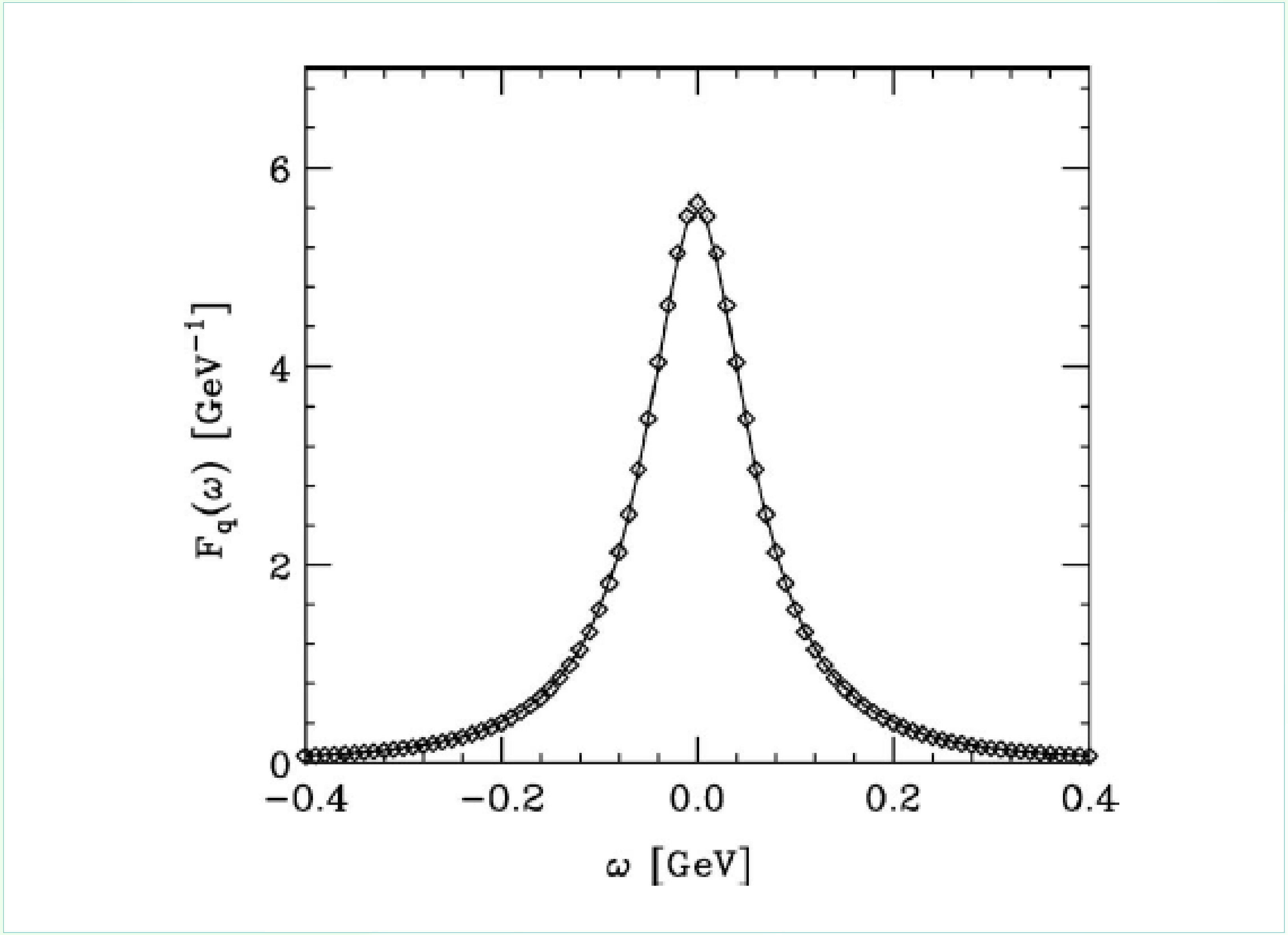

Real part of the optical potential

We account for the spectrum modification by

$$\boxed{f_{\mathbf{q}}(\omega - \omega') \to f_{\mathbf{q}}(\omega - \omega' - U_V).}$$

This procedure is similar to that from the Fermi gas model to introduce the binding energy in the argument of δ(...).

$$\boxed{U_V = U_V(t_{\mathrm{kin}})}$$

$$\boxed{t_{\mathrm{kin}} = \frac{E_{\mathbf{k}}^2(1-\cos\theta)}{M + E_{\mathbf{k}}(1-\cos\theta)}}$$

Optical potential by Cooper *et al.*

Widely used in proton scattering, fit of the scattering solutions of the Dirac equation to the data for

- elastic cross section,
- analyzing power,
- spin rotation function,

available for protons of kinetic energy $29 \leq t_{kin} \leq 1040$ MeV..

Optical potential by Cooper *et al.*

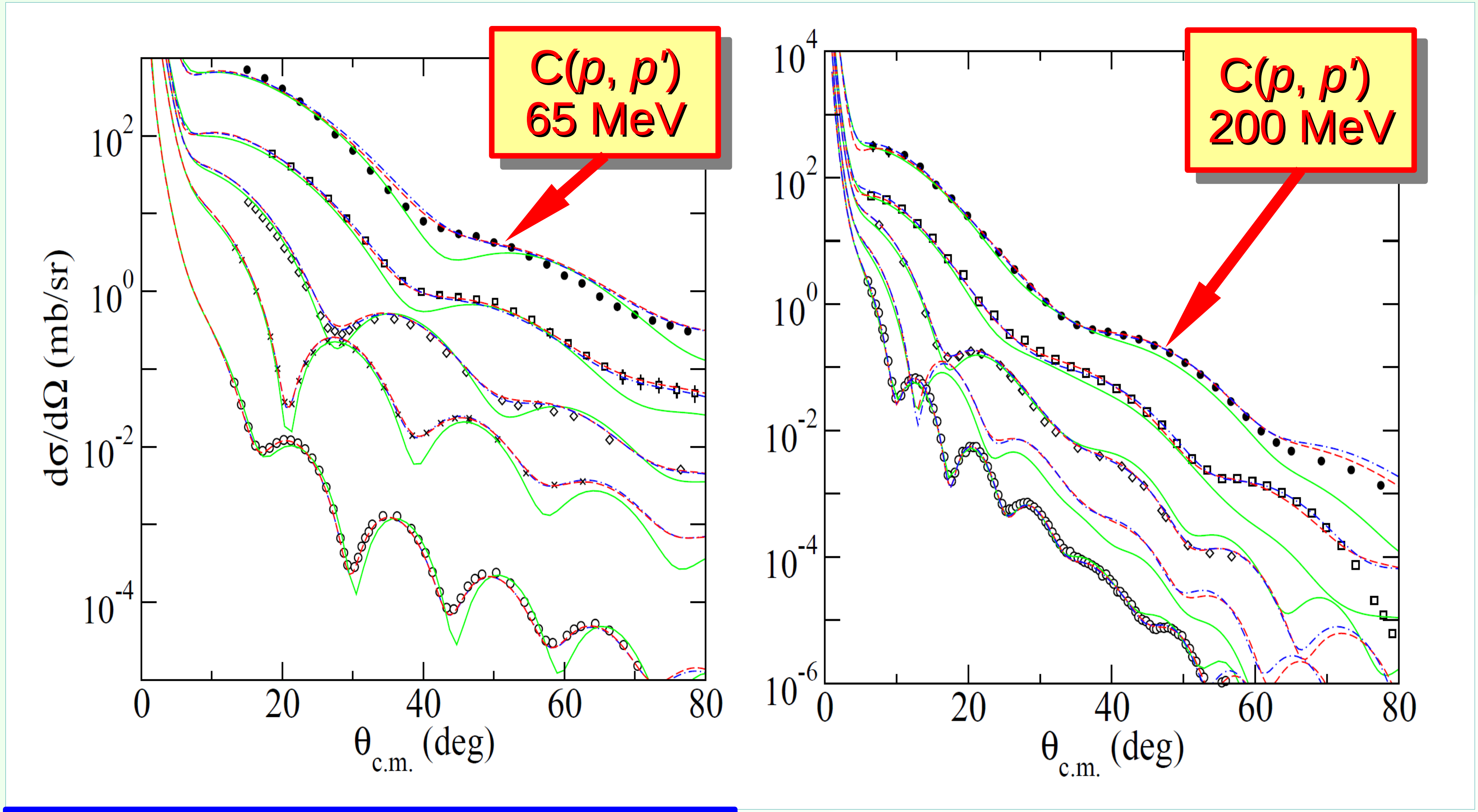

Deb *et al.*, PRC 72, 014608 (2005)

Optical potential by Cooper *et al.*

Dirac phenomenology

$$\boxed{(\gamma^\mu p_\mu - \gamma^0 V + M + S)\psi = 0}$$

Optical potential as a modification of the on shell energy

$$\boxed{E_p + U = \sqrt{(M+S)^2 + \mathbf{p}^2} + V}$$

We are interested in the average quantity, $U = U(t_{\mathrm{kin}})$

$$\boxed{\int d^3 r \rho(r) E'_{\mathrm{tot}} = E_{\mathbf{p}'} + U}$$

Optical potential by Cooper *et al.*

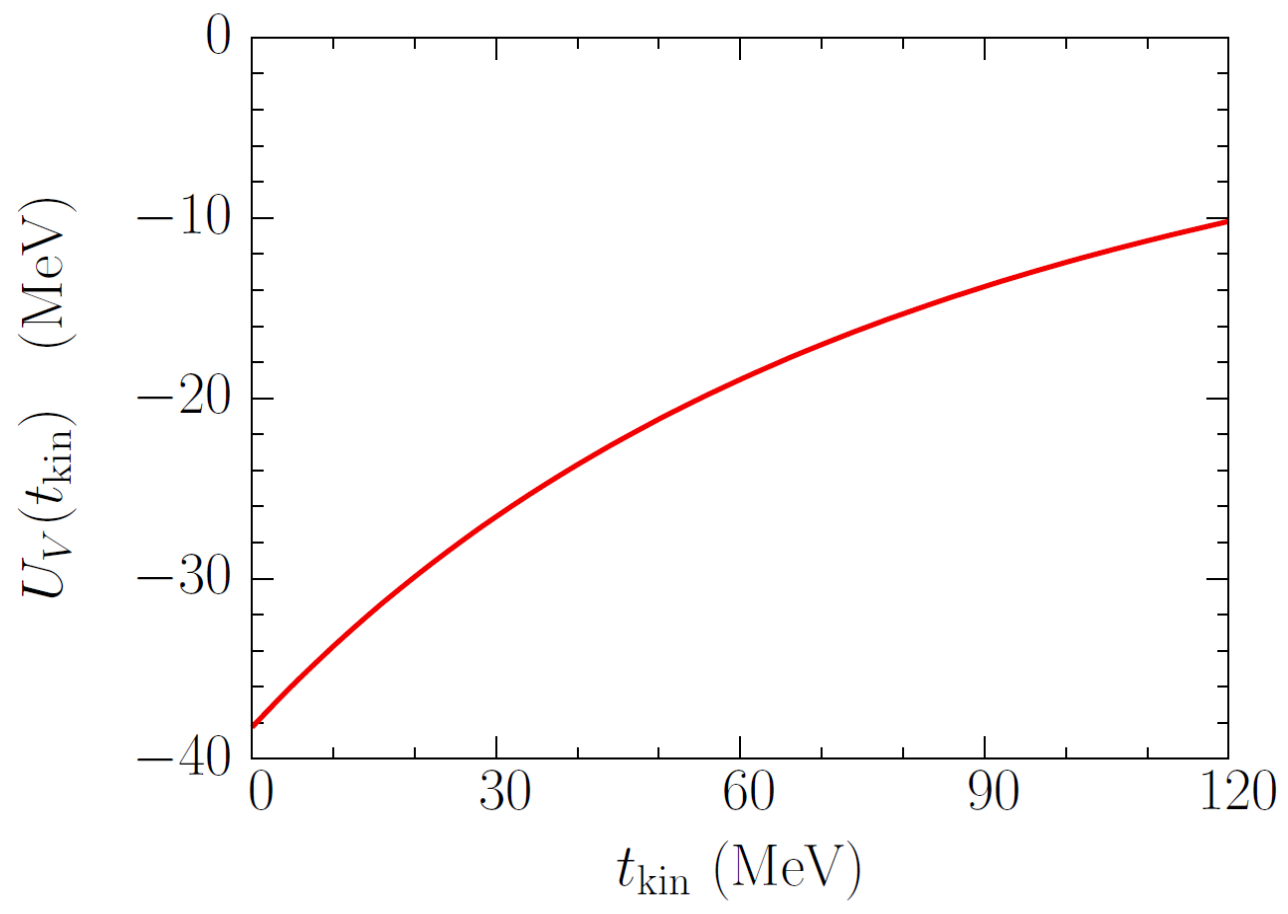

obtained from
Cooper *et al.*, PRC 47, 297 (1993)

Simple comparison

Real part of the OP

- acts in the final state
- shifts the QE peak
  to low ω at low $|\mathbf{q}|$
  (to high ω at high $|\mathbf{q}|$)

Binding energy in RFG

- acts in the initial state
- shifts the QE peak to high ω

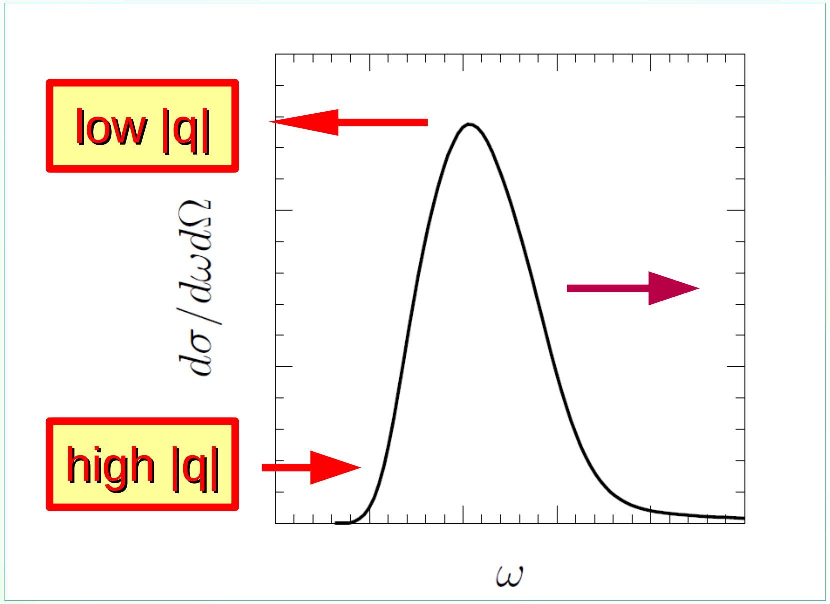

Comparison to C(*e*, *e'*) data

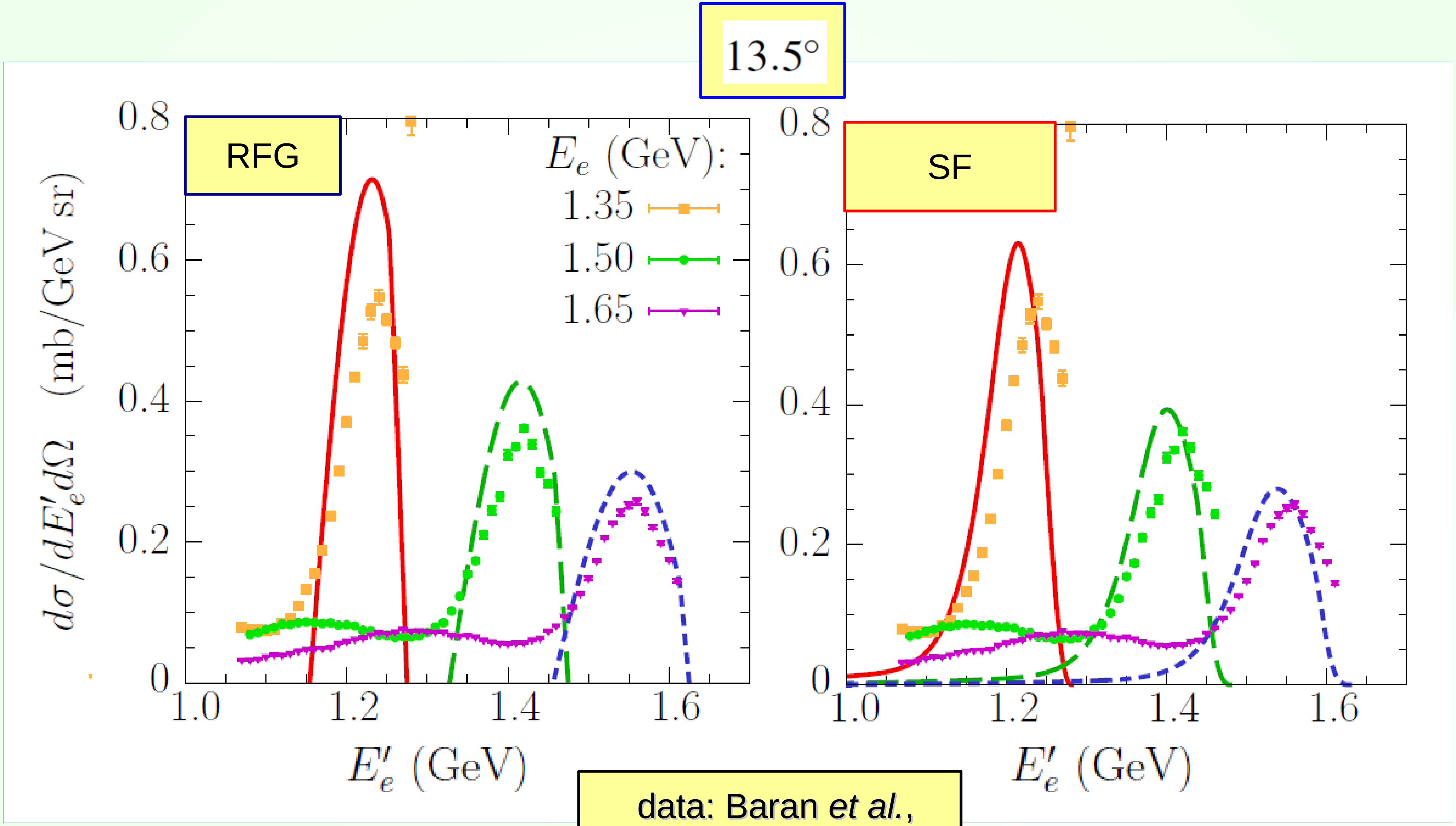

data: Baran *et al.*,
PRL 61, 400 (1988)

Comparison to C(e, e') data

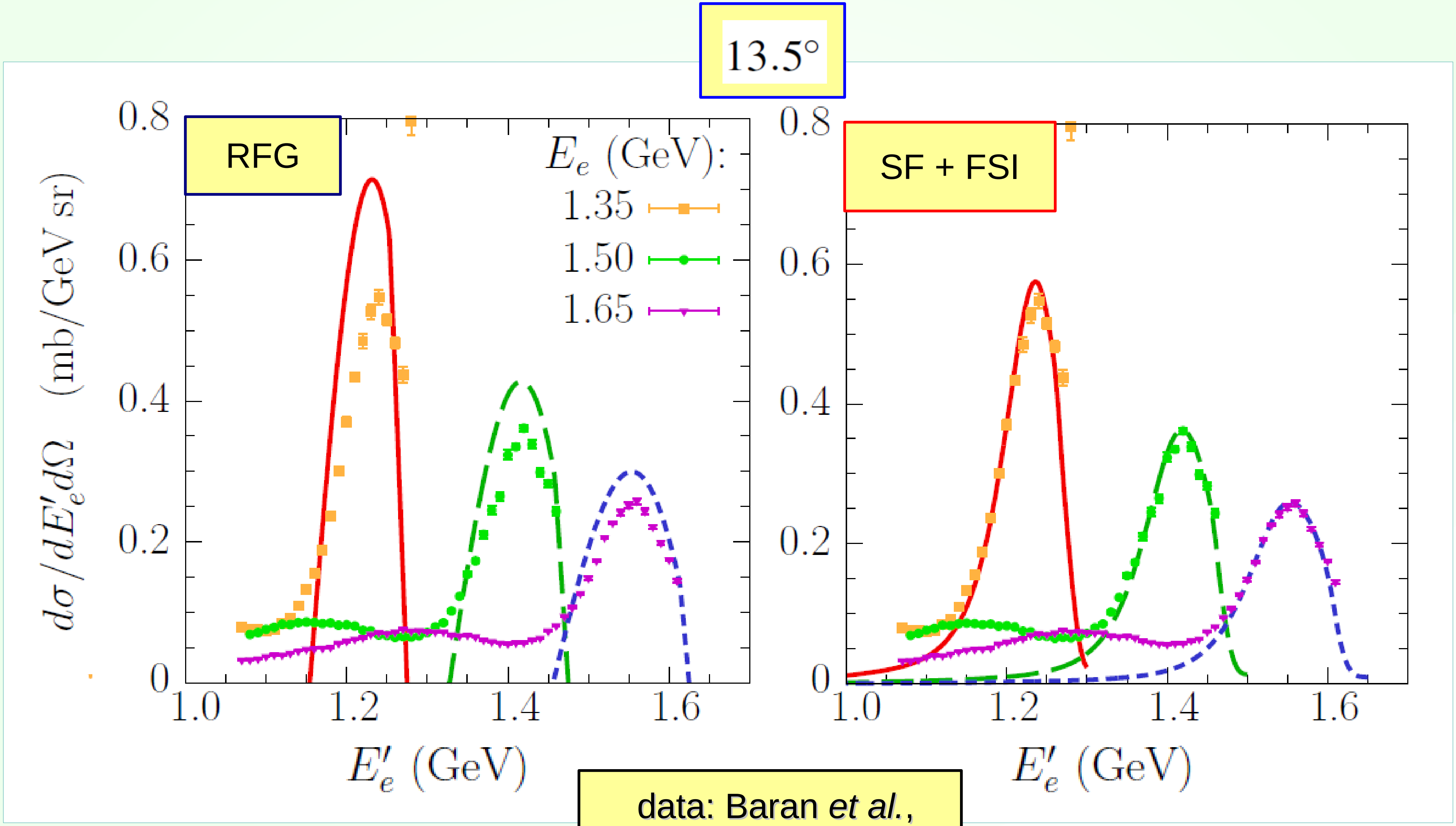

data: Baran *et al.*, PRL 61, 400 (1988)

Importance of quasielastic scattering

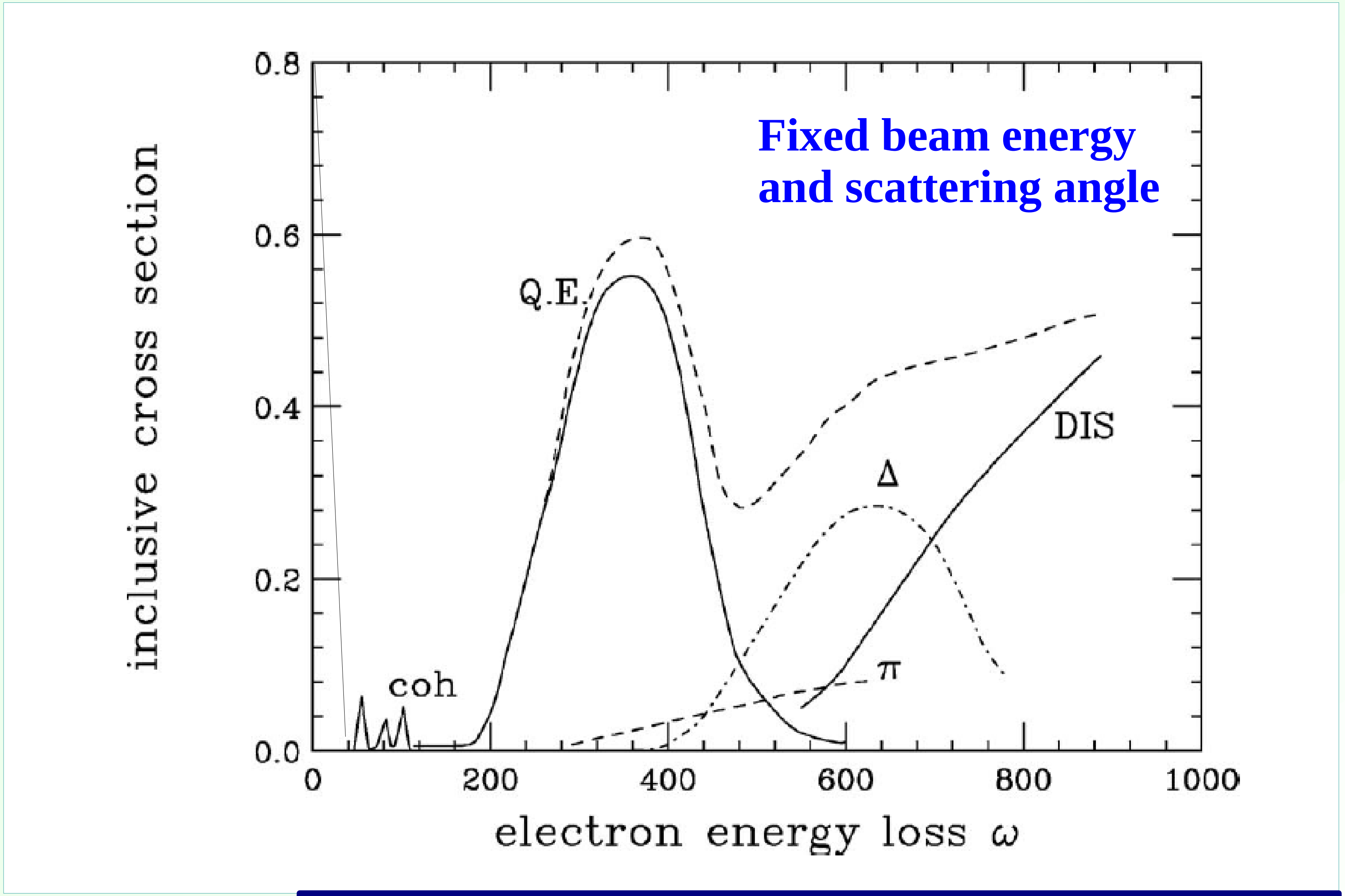

adopted from Benhar *et al.*, RMP 80, 189 (2008)

Compared calculations

A.M.A, O. Benhar and M. Sakuda,
Phys. Rev. D 91, 033005 (2015)
[arXiv:1404.5687]

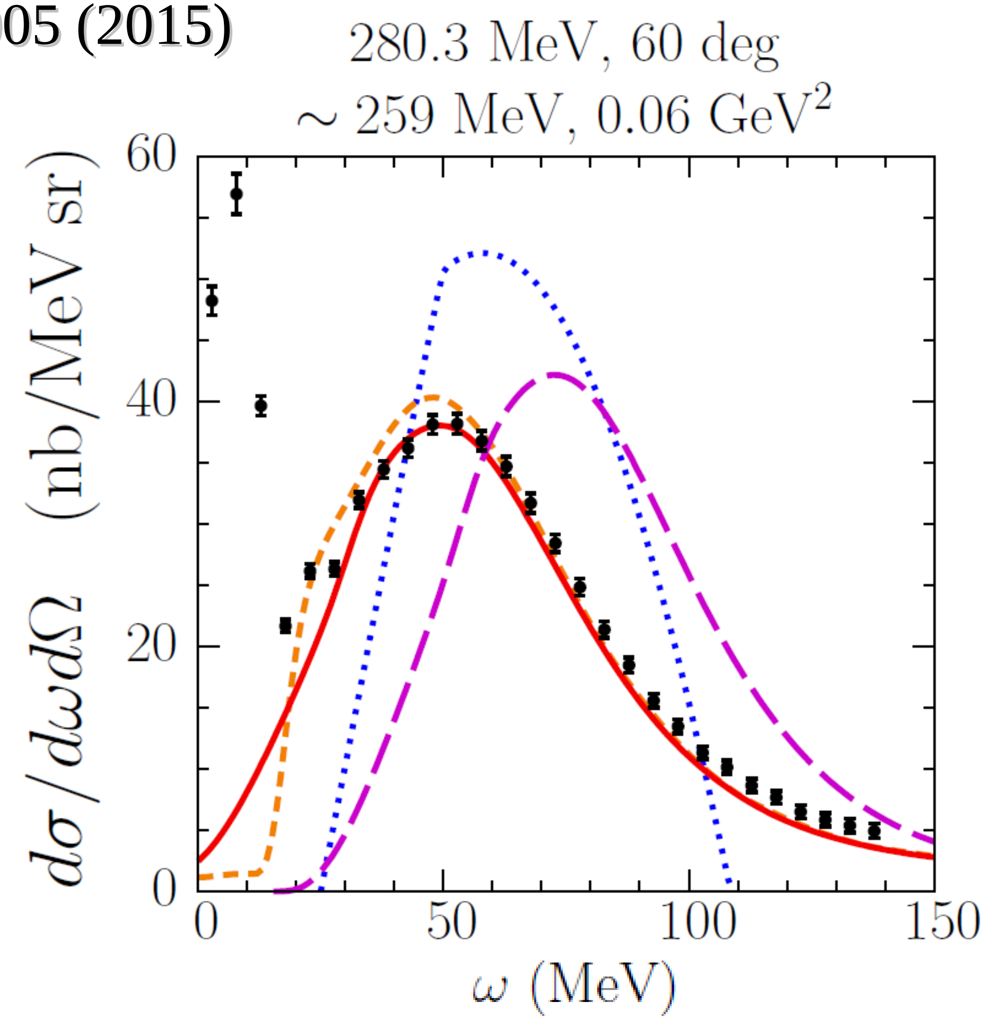

RFG model
ε = 25 MeV
p_F = 221 MeV

SF calculation without FSI

SF calculation, LDA treatment of Pauli blocking

SF calculation, step function

Compared calculations

Calcs. include QE by 1-body current only

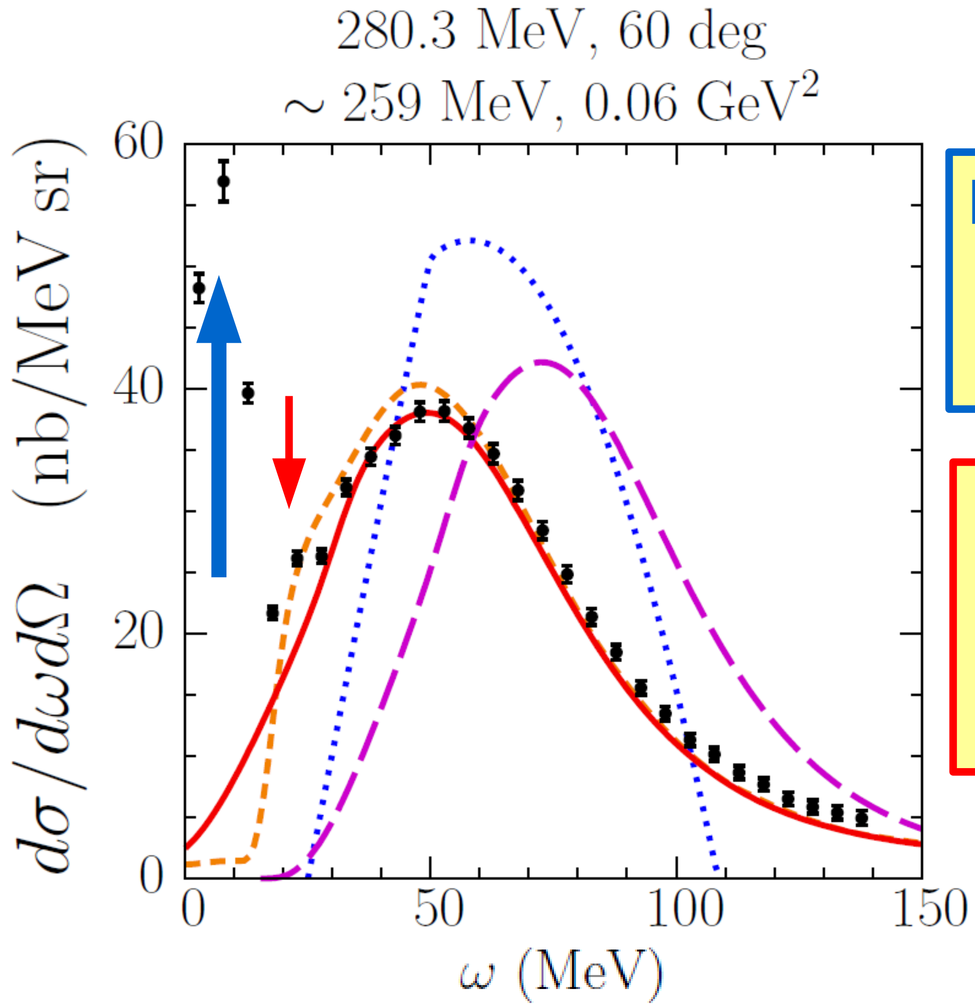

Elastic scattering and excitation of low-E_x levels

Giant resonance
E_x = 22.6 MeV,
Γ = 3.2 MeV

Comparisons to C(*e*,*e*′) data

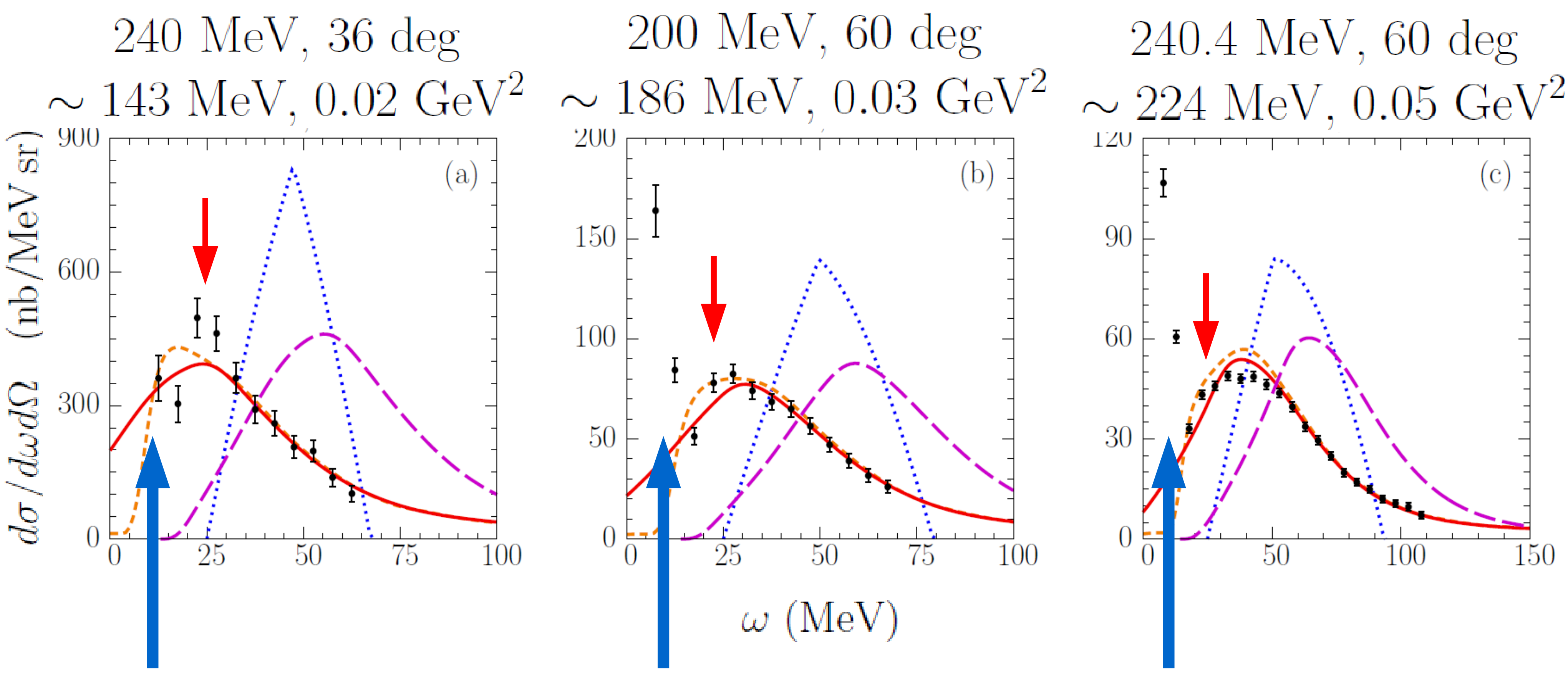

Barreau *et al.*,
NPA 402, 515 (1983)

Comparisons to C(*e*,*e'*) data

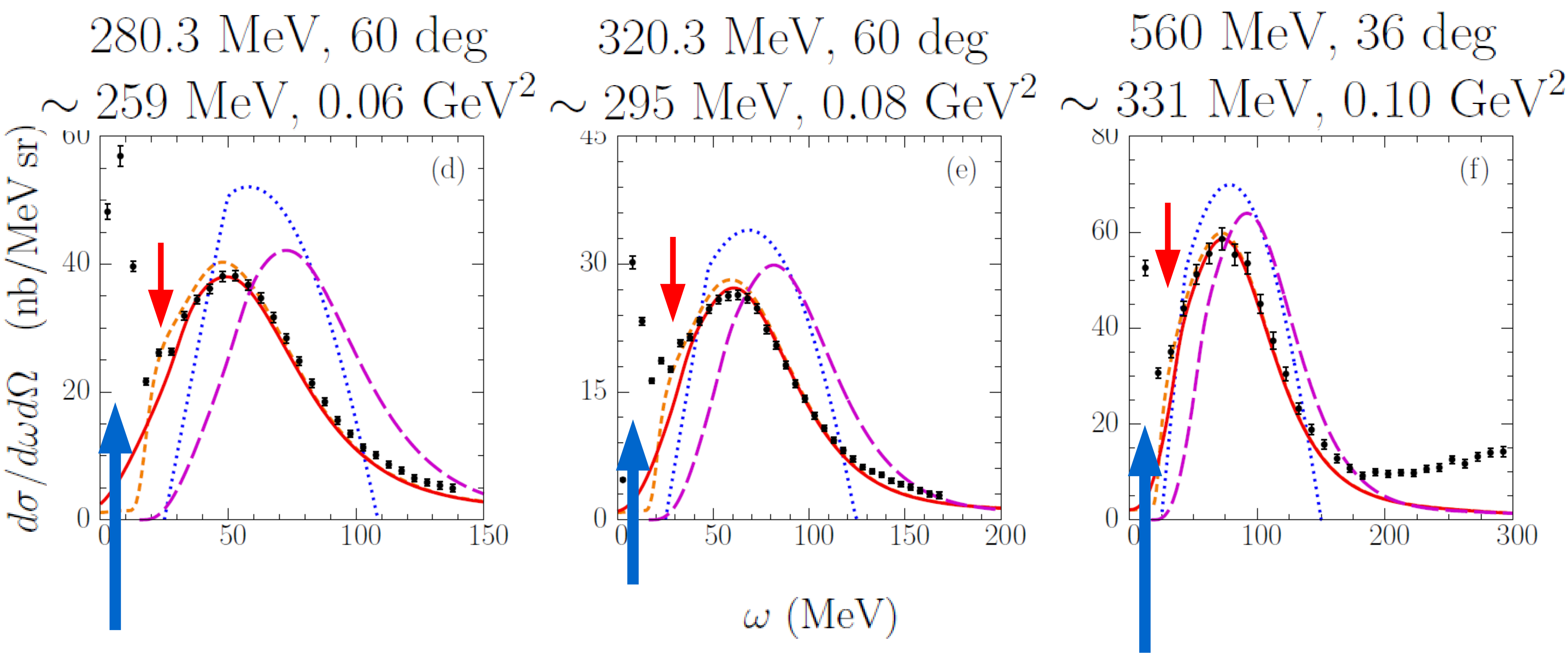

Barreau *et al.*,
NPA 402, 515 (1983)

Comparisons to C(e,e') data

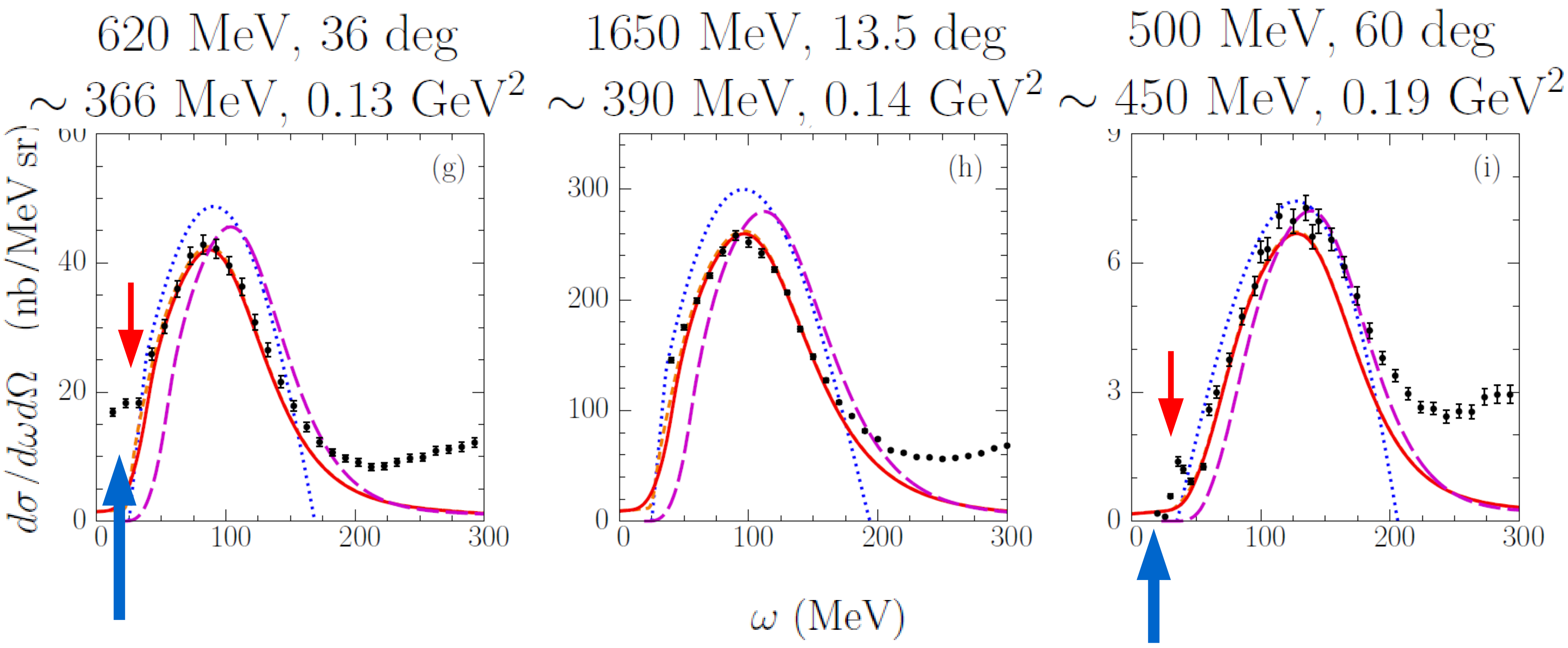

Barreau *et al.*,
NPA 402, 515 (1983)

Baran *et al.*,
PRL 61, 400 (1988)

Whitney *et al.*,
PRC 9, 2230 (1974)

Comparisons to C(e,e') data

The supplemental material of PRD 91,033005 (2015)
shows comparisons to the data sets collected
at **54 kinematical setups**

- energies from ~160 MeV to ~4 GeV,
- angles from 12 to 145 degrees,
- at the QE peak, the values of momentum transfer from ~145 to ~1060 MeV/c and $0.02 \leq Q^2 \leq 0.86$ (GeV/c)^2 .

Kin. Reconstruction of E_ν = 600 MeV

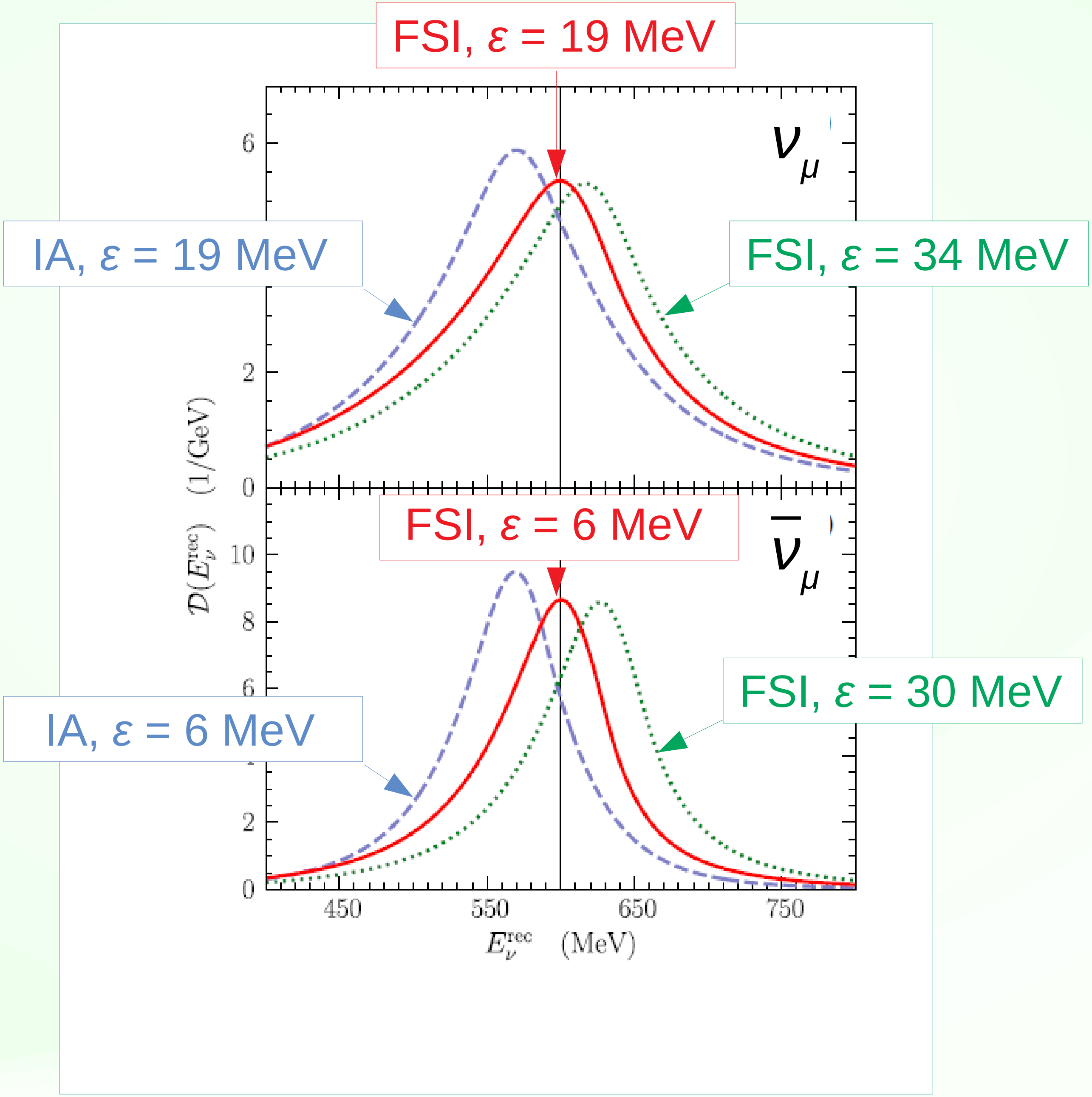

Kinematic E_ν Reconstruction

E_ν	200	400	600	800	1000
FSI, ν_μ, $\epsilon = 19$ MeV	211	401	600	799	998
IA, ν_μ, $\epsilon = 19$ MeV	173	370	570	770	970
FSI, ν_μ, $\epsilon = 34$ MeV	229	419	617	816	1015
FSI, $\bar{\nu}_\mu$, $\epsilon = 6$ MeV	210	402	600	799	999
IA, $\bar{\nu}_\mu$, $\epsilon = 6$ MeV	172	369	569	769	969
FSI, $\bar{\nu}_\mu$, $\epsilon = 30$ MeV	239	429	627	826	1025
FSI, ν_e, $\epsilon = 19$ MeV	206	401	599	799	998
FSI, $\bar{\nu}_e$, $\epsilon = 6$ MeV	206	402	600	799	999

$\varepsilon = \varepsilon(E_\mu, \cos\theta)$

vs.

$\varepsilon = \text{const}$

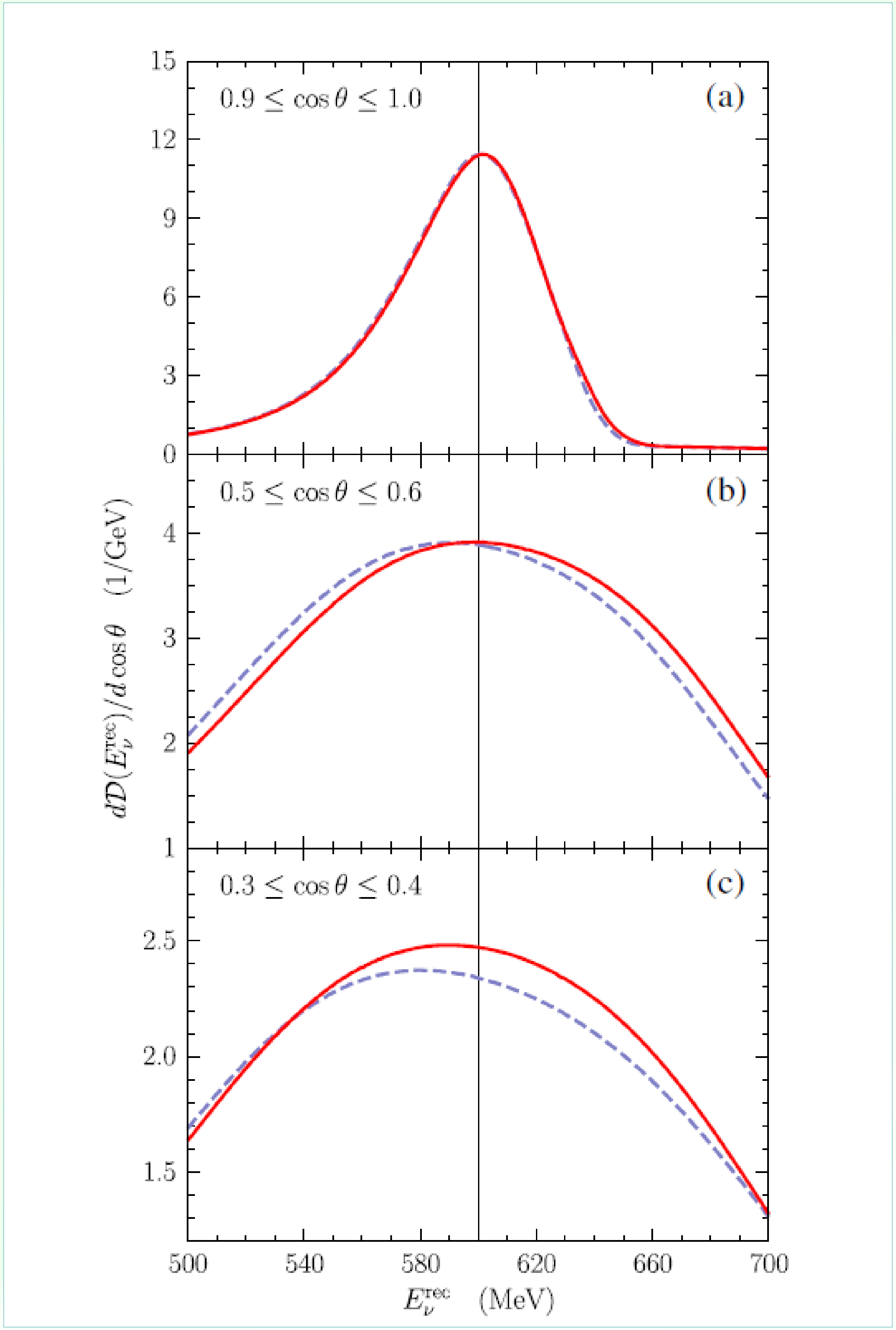

CCQE MINERvA data

SF calculations with FSI

vs.

SF calculation without FSI

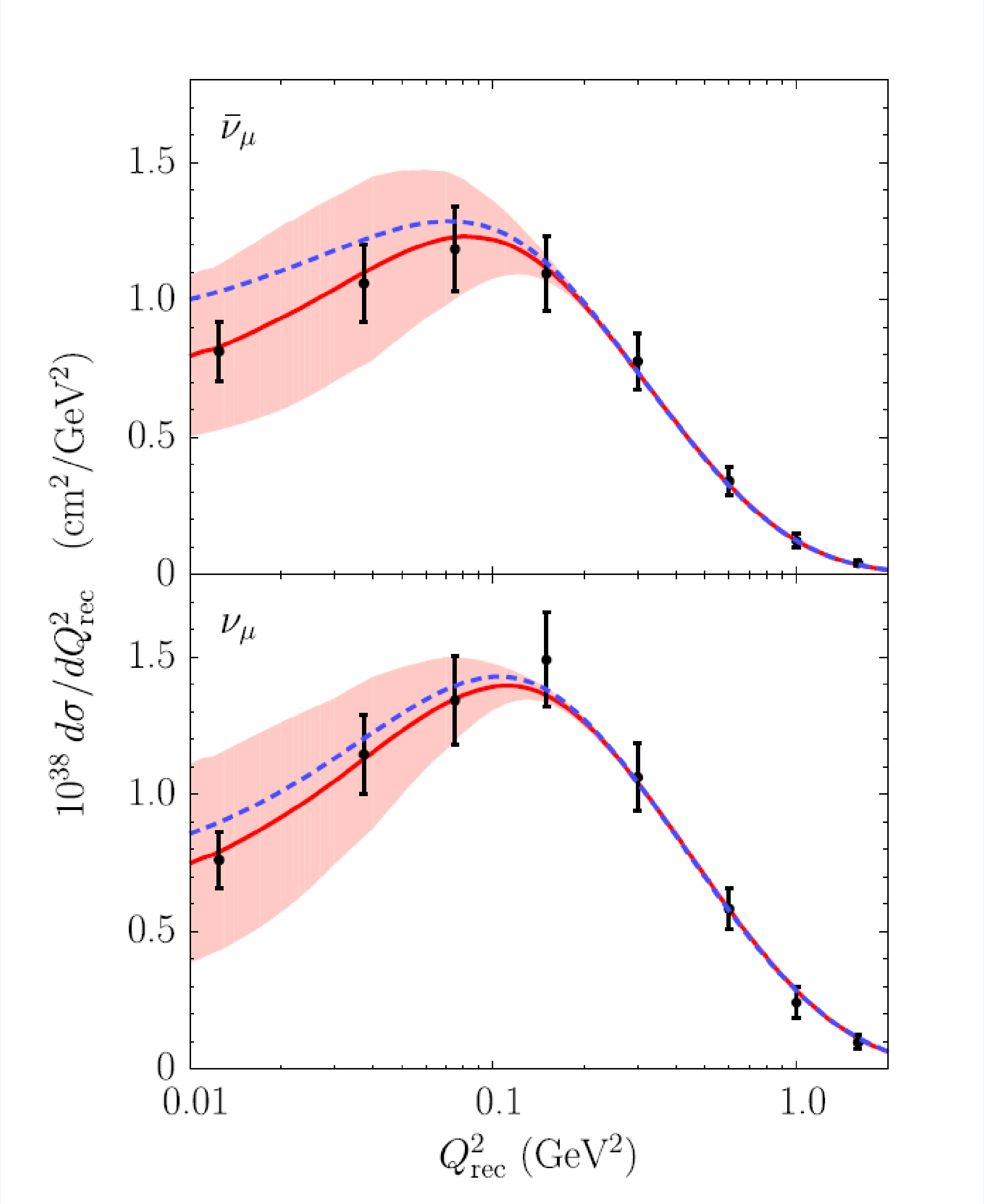

Fields *et al.*, PRL 111, 022501 (2013)

A. M. A., PRD 92, 013007 (2015)

Fiorentini *et al.*, PRL 111, 022502 (2013)

CCQE MINERvA data

TABLE I. Fit results to the CC QE MINERvA data.

	antineutrino	neutrino	combined fit
	including theoretical uncertainties:		
M_A (GeV)	1.16 ± 0.06	1.17 ± 0.06	1.16 ± 0.06
χ^2/d.o.f.	0.38	1.33	0.93
	neglecting theoretical uncertainties:		
M_A (GeV)	1.15 ± 0.10	1.15 ± 0.07	1.13 ± 0.06
χ^2/d.o.f.	0.44	1.38	1.00
	neglecting FSI ($M_A = 1.16$ GeV):		
χ^2/d.o.f.	2.49	2.45	2.42

Energy reconstruction

Kinematic reconstruction

In quasielastic scattering off free nucleons, $\bar{\nu} + p \rightarrow l + n$ and $\nu + n \rightarrow l + p$, we can deduce the neutrino energy from the charged lepton's kinematics.

No need to reconstruct the nucleon kinematics.

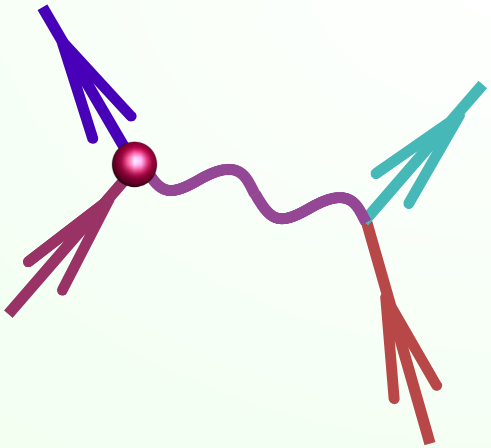

E' and θ known

$$E = \frac{ME' + \text{const}}{M - E' + |\boldsymbol{k}'| \cos\theta}$$

Kinematic reconstruction

In nuclei the reconstruction becomes an approximation due to the binding energy, Fermi motion, final-state interactions, two-body interactions etc.

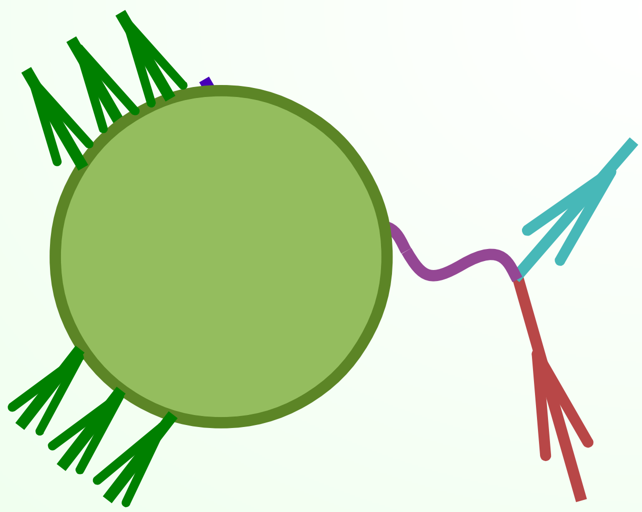

E' and θ known

$$E \simeq \frac{(M-\epsilon)E' + \text{const}}{M-\epsilon-E'+|\boldsymbol{k}'|\cos\theta}$$

Unknown monochromatic beam

Consider the simplest (unrealistic) case:

the beam is monochromatic but its energy is unknown and has to be reconstructed

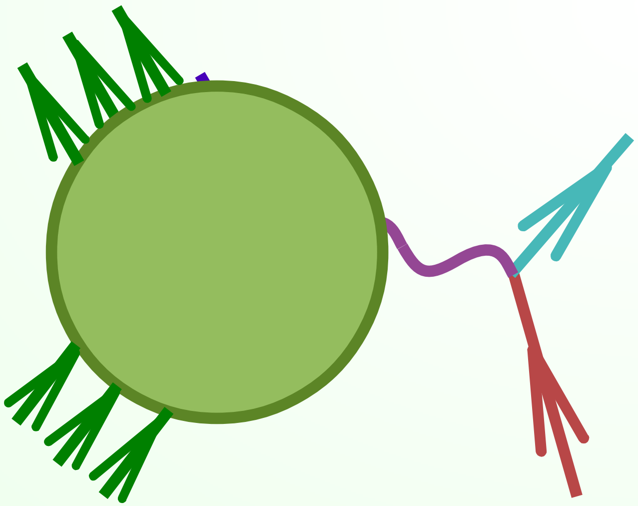

E' and θ known

$E = ?$

PoS(NuFact2014)004

“Unknown” monochromatic e^- beam

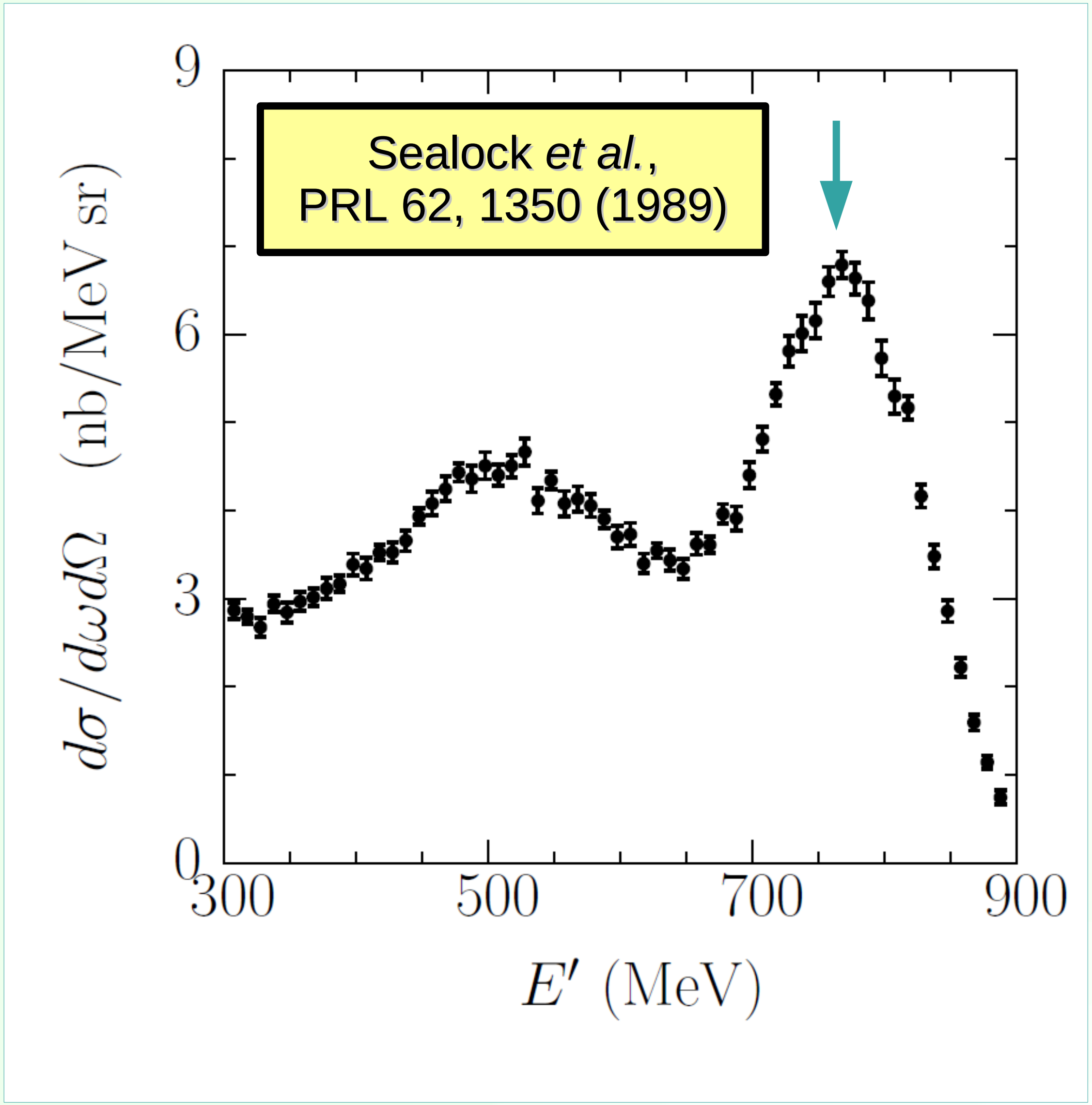

$E' = 768$ MeV
$\theta = 37.5$ deg
$\Delta E' = 5$ MeV

"Unknown" monochromatic e^- beam

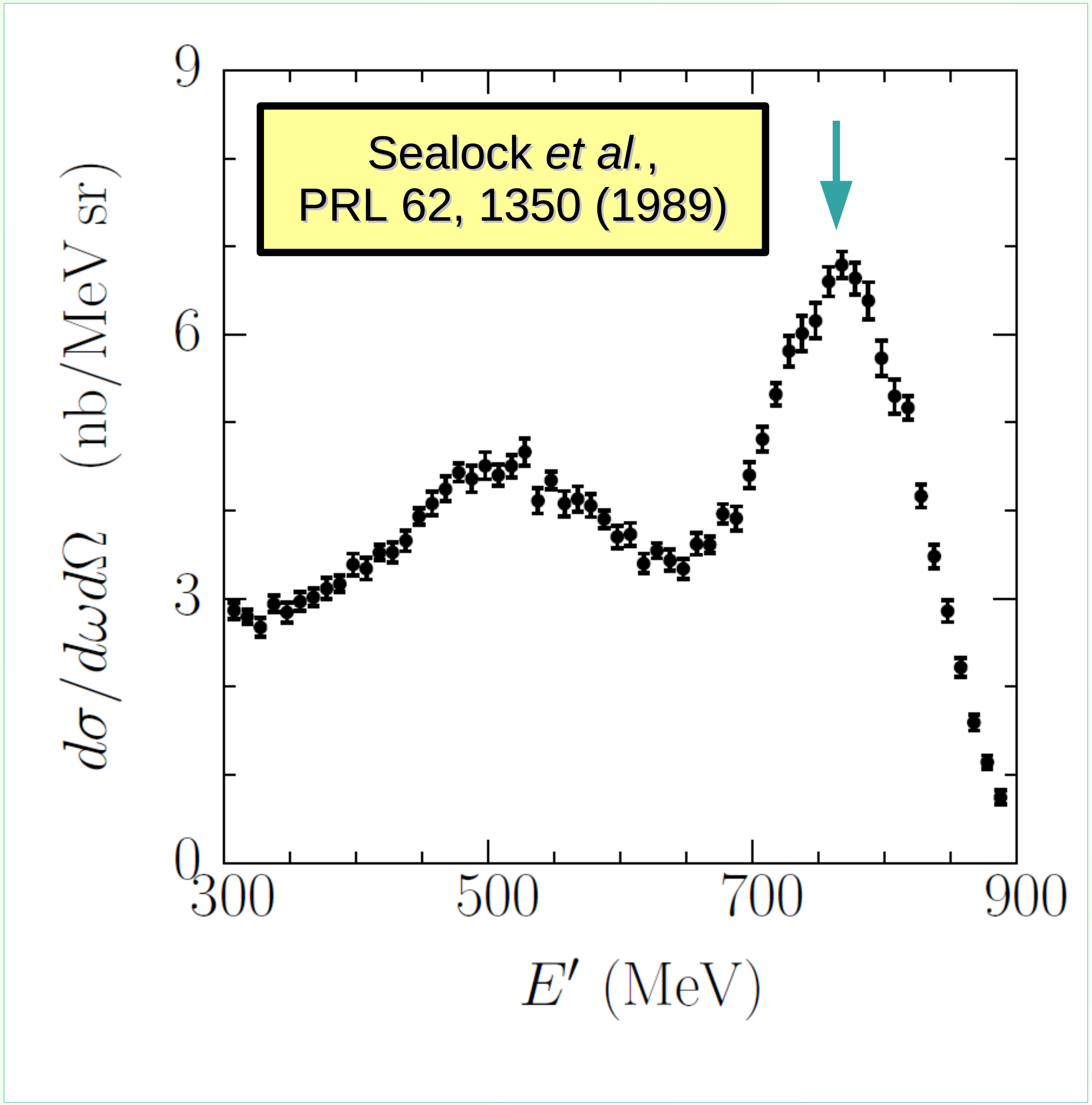

$$E' = 768 \text{ MeV}$$
$$\theta = 37.5 \text{ deg}$$
$$\Delta E' = 5 \text{ MeV}$$

for $\epsilon = 25$ MeV
$$E = 960 \text{ MeV}$$
$$\Delta E = 7 \text{ MeV}$$

“Unknown” monochromatic e^- beam

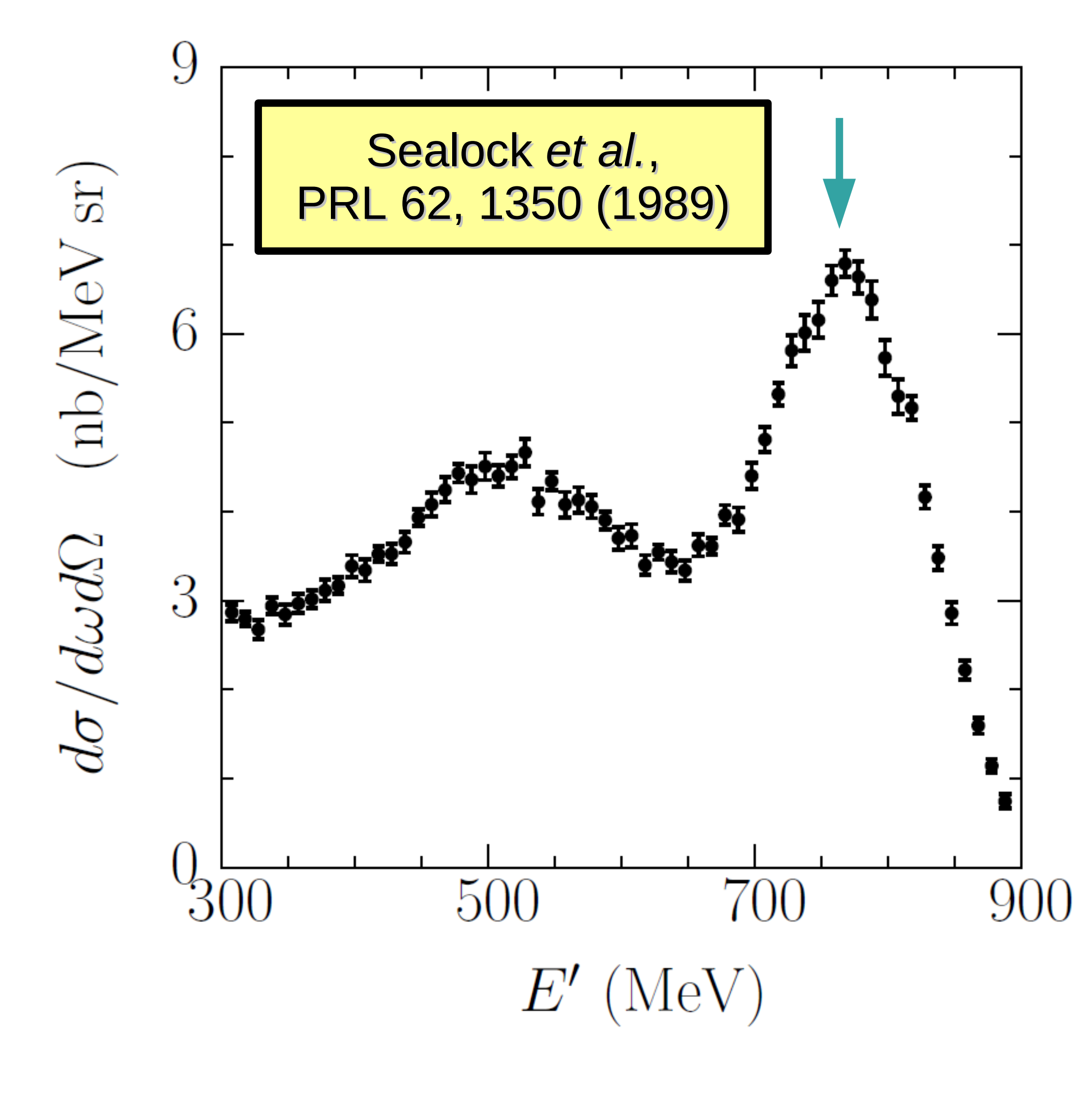

$E' = 768$ MeV
$\theta = 37.5$ deg
$\Delta E' = 5$ MeV

for $\epsilon = 25$ MeV
$E = 960$ MeV
$\Delta E = 7$ MeV

true value
$E = 961$ MeV

“Unknown” monochromatic e^- beam

θ (deg)	37.5	37.5	37.1	36.0	36.0
E' (MeV)	976	768	615	487.5	287.5
$\Delta E'$ (MeV)	5	5	5	5	2.5

Assuming $\epsilon = 25$ MeV

rec. E	1285 ± 8	960 ± 7	741 ± 7	571 ± 6	333 ± 3
true E	1299	961	730	560	320

“Unknown” monochromatic e^- beam

θ (deg)	37.5	37.5	37.1	36.0	36.0
E' (MeV)	976	768	615	487.5	287.5
$\Delta E'$ (MeV)	5	5	5	5	2.5

Appropriate ϵ value?

true E	**1299**	**961**	**730**	**560**	**320**
ϵ	**33 ± 5**	**26 ± 5**	**16 ± 5**	**16 ± 3**	**13 ± 3**

Sealock et al., PRL 62, 1350 (1989)

O'Connell *et al.*, PRC 35, 1063 (1987)

Barreau *et al.*, NPA 402, 515 (1983)

“Unknown” monochromatic e^- beam

θ (deg)	37.5	37.5	37.1	36.0	36.0
E' (MeV)	976	768	615	487.5	287.5
$\Delta E'$ (MeV)	5	5	5	5	2.5

Appropriate ϵ value?

true E	**1299**	**961**	**730**	**560**	**320**
ϵ	33 ± 5	26 ± 5	16 ± 5	16 ± 3	13 ± 3

different $E \equiv$ different $Q^2 \equiv$ different θ
$\rightarrow$ different ϵ

“Unknown” monochromatic e^- beam

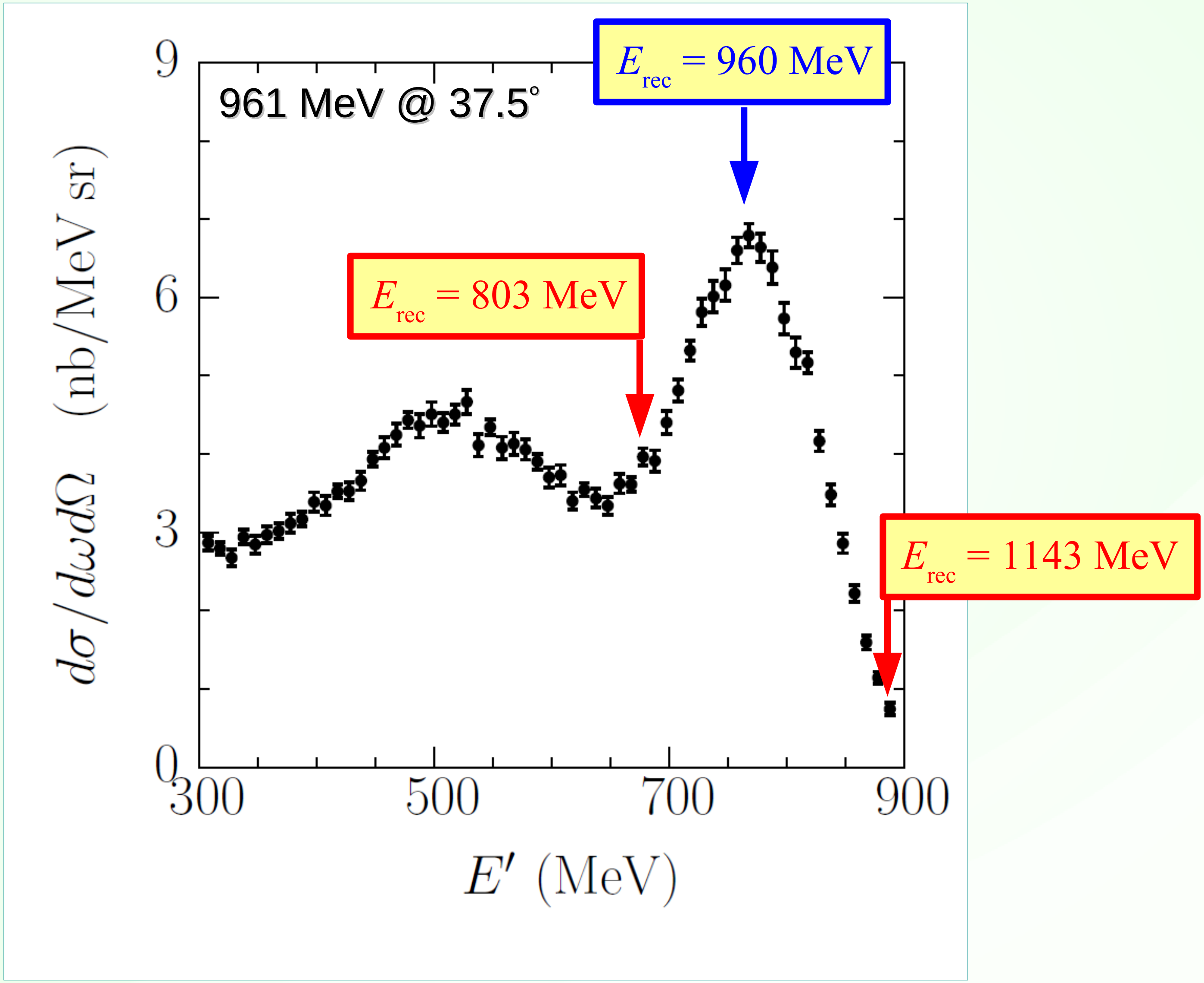

Summary

- An accurate description of nuclear effects, including final-state interactions, is crucial for an **accurate reconstruction of neutrino energy**.
- The spectral function formalism can be used in Monte Carlo simulations to **improve the accuracy** of description of nuclear effects.
- Effect of final state interactions on lepton distributions is important at **low momentum transfers**.

Backup slides